RESEARCH & DEVELOPMENT

Predicting Lane Change Intensity within Urban Interchange Influence Areas (IIA)

Institute for Transportation Research and Education (ITRE)
North Carolina State University
Nagui M. Rouphail, PhD
Principal Investigator

NCDOT Project 2019-29

November, 2020

Technical Report Documentation Page

1. Report No. **NCDOT/NC/2019-29**	2. Government Accession No.	3. Recipient's Catalog No.
4. Title and Subtitle **Predicting Lane Change Intensity within Urban Interchange Influence Areas (IIA)**		5. Report Date **November 2020**
		6. Performing Organization Code **ITRE / NC State University**
7. Author(s) **Nagui M. Rouphail, Ishtiak Ahmed, Alan Karr, and Thomas Chase**		8. Performing Organization Report No.
9. Performing Organization Name and Address **Institute for Transportation Research and Education** **North Carolina State University** **Centennial Campus Box 8601** **Raleigh, NC**		10. Work Unit No. (TRAIS)
		11. Contract or Grant No. **NCDOT RP2019-29**
12. Sponsoring Agency Name and Address **North Carolina Department of Transportation** **Research and Analysis Group** **104 Fayetteville Street** **Raleigh, North Carolina 27601**		13. Type of Report and Period Covered **Final Report** **August 2018 to July 2020**
		14. Sponsoring Agency Code **NCDOT/NC/2019-29**
Supplementary Notes:		

16. **Abstract**

This research project provides NCDOT with a tool for predicting freeway lane changes at interchange influence areas (IIAs). The tool estimates the total number of lane changes on a segment using two different models, one that assumes knowledge of the minimum number of lane changes (MinLaneChanges), and a second one that does not. A total of 15 sites were videotaped using a combination of ground based and drone fitted cameras. On average, the observed number of lane changes across sites was 1,373 lane changes/hour (lc/h). The range for the first model with known MinLaneChanges varied from a low of 251 to a high of 3,798 lc/h, and for the second model absent MinLaneChanges from 343 to 3,816 lc/h. Generally low rates of lane changes were associated with low values of MinLaneChanges, short segment lengths, low vehicle miles of travel (VMT) and low or congested average speed. In the first model, when MinLaneChanges fell below 450 lc/h, the total lane changes per hour were only about 22% of those occurring when MinLaneChanges exceeded 450 lc/h. The two models have been implemented in a web-based tool, including s a computational engine, a user guide and an input variables calculator. In addition, the team tested a proposed geometric treatment intended to reduce lane change frequency at the I-40EB weaving segment between Harrison Blvd. and Wade Avenue. The testing methodology was microsimulation using VISSIM. The model was calibrated based on field observed OD flow distributions and travel times. This analysis revealed that the treatment generated total travel time savings of 16.2 veh-hours per clock hour, which is applicable to two hours in the PM peak on a typical weekday. The treatment also reduced the simulated overall lane change frequency by a significant 22%.

17. Key Words **Lane change, interchange influence area, predictive model, lane change treatment**	18. Distribution Statement **Unlimited**

19. Security Classification (of this report) **Unclassified**	20. Security Classification (of this page) **Unclassified**	21. No. of Pages: **60**	22. Price

Form DOT F 1700.7 (8-72) **Reproduction of completed page authorized**

DISCLAIMER

The contents of this report reflect the views of the authors and not necessarily the views of the North Carolina Department of Transportation. The authors are responsible for the facts and the accuracy of the data presented herein. The contents do not necessarily reflect the official views or policies of the North Carolina Department of Transportation or North Carolina State University at the time of publication. This report does not constitute a standard, specification, or regulation.

ACKNOWLEDGEMENTS

The research team wishes to thank the many individuals at ITRE, NCSU, and at the North Carolina Department of Transportation who contributed to the project.

EXECUTIVE SUMMARY

This research project aims at providing the North Carolina Department of Transportation with a computational tool for predicting freeway lane change intensity near interchange influence areas (IIAs). The intent was to use data that are readily available to traffic engineers and analysts in the state to generate those predictions. The proposed model estimates the total number of lane changes on a freeway segment using two different sub-models, one that assumes knowledge of the number of the mandatory or minimum number of lane changes (MinLaneChanges), and a second model that does not. The first model is applicable to existing interchange areas where ramp volumes are known, while the second can be used for new interchange analyses at the planning stage. Data needed to develop the prediction tool included both geometric and traffic stream variables. A total of fifteen sites in North Carolina were videotaped using a combination of ground based and drone fitted cameras. Lane changes were tracked using video tracking software in 5 minute time intervals, subsequently expanded to hourly rates.

Overall, the average observed number of lane changes across all sites and time intervals was 1,373 lane changes/hour (lc/h). The range of the response variable for the first model with known MinLaneChanges varied from a low of 251 to a high of 3,798 lc/h, and for the second model absent MinLaneChanges from 343 to 3,816 lc/h. Generally speaking, low rates of lane changes were associated with low values of MinLaneChanges, short segment lengths, low vehicle miles of travel (VMT) and low average speed. The first explanatory variable in the tree absent MinLaneChanges was the actual segment length, with longer segments generating higher lane change rates. Interestingly, we found from the first model, that when MinLaneChanges fell below 450 lc/h, the total lane changes per hour were only about 22% of those occurring when MinLaneChanges exceeded 450 lc/h. Furthermore our observations of the data indicated that lane change frequency decreased as the level of congestion increased. The two models have been implemented in a prototype web-based tool, which includes a computational engine, along with a user guide and an input variables calculator. Further work on testing and validating the web tool will resume when physical access to the NC State University campus facilities is permitted.

In addition, the research team tested a proposed geometric treatment that was intended to reduce lane change frequency at the I-40EB weaving segment between Harrison Blvd. and Wade Avenue. The testing methodology was microsimulation using the VISSIM microsimulation model. The model was calibrated based on observed Origin Destination (OD) flow distributions and OD travel times measured from field Bluetooth units at the site. Key findings from this analysis revealed that the treatment generated total travel time saving of 16.2 veh-hours per clock hour, which is applicable to two hours in the PM peak on a typical weekday. The treatment did reduce the simulated overall lane change frequency by a significant 22%.

TABLE OF CONTENTS

LIST OF FIGURES

LIST OF TABLES

CHAPTER 1 : INTRODUCTION

1.1 Background and Motivation

Empirical evidence suggests that excessive lane changing at freeway interchanges in NC urban areas results in increased turbulence, decreased safety, and high levels of acceleration and deceleration cycles with the potential for emission increases. When operating in near capacity conditions, those mostly *discretionary* lane changes may result in a bottleneck activation and associated (and unnecessary) drops in mobility quality of service. One obstacle to predicting lane changes empirically is the difficulty in measuring them in the field. The research used innovative methods for both data collection – using mostly drone videos—and extraction using third party software to generate a unique lane change database. As a result, this project has revealed the relationship between lane change intensity at interchanges on the one hand and traffic conditions and site geometric attributes on the other. Based on those findings, the research also provides a method for assessing the effectiveness of operational treatments aimed at reducing lane-change disturbances near interchange areas. This portion of the research utilized microsimulation to demonstrate the validity of the approach.

In a recently completed study for NCDOT on the systematic identification of recurring freeway bottlenecks, the top 12 identified bottlenecks in the Research Triangle region occurred in an interchange influence area (IIA). With anticipated traffic demand to continue to be on an upward trajectory in NC and with little to no likelihood of major capacity additions in the foreseeable future, approaches that can improve the efficient use of the available roadway capacity are sorely needed. This research was aimed at both understanding how lane change intensity is motivated by traffic and interchange configuration, for example near basic, merge or diverge segments, and to assess methods for mitigating the deleterious effect of lane changes on interchange mobility quality of service. This will assist in future planning and design of interchanges and for the identification of lane change “hot spots” that should be considered for treatments. In fact, our literature review has concluded that no previous study has attempted to model the lane change intensity at urban interchange areas in a comprehensive manner, mainly due to the lack of observation at multiple sites. Even recent studies regarding lane change observations relied on manual extraction of lane-change events from the high-resolution data feed which restricts the usability of detailed information in predicting lane-change intensity. In general, the focus has been on the analysis of lane changes, rather than their quantification.

Cognizant of the need for NCDOT to have access to a practical tool to make such predictions, the research team has developed a web-based prediction tool requiring mostly available input data items to accomplish that task. Both a user guide and a spreadsheet calculator have been developed to produce some of the required tool’s inputs in the event they are not readily available to the end user supplement the tool.

1.2 Research Objectives

The primary objective of this research was to develop a practical tool for NCDOT to enable the prediction of the expected intensity of mandatory and discretionary lane changes at an IIA, based exclusively on data sources that are readily available to the department. This task was executed based on extensive observations and recording of lane changes in the field.

A second objective was to ascertain whether changes in signing, markings or other traveler information near the IIA could induce fewer discretionary lane changes and thus reduce unnecessary traffic turbulence near interchanges. Originally, this objective was to be carried out in simulation, followed --if it met the spot mobility criteria with a pilot field test. As will be demonstrated in Chapter 6 of this report, the simulated treatment based on a calibrated VISSIM model of a weaving segment on I-40, was shown to reduce the propensity of excessive lane changes, but did not meet the spot mobility criteria for implementation.

1.3 Scope and limitations of the Study

Lane change studies are typically based on the use of either microscopic (individual vehicle based) or macroscopic (flow based) variables. The NGSIM project and the Naturalistic Driving Study exemplify the first class. For example, NGSIM generates vehicle trajectories to analyze car following and lane change patterns on freeways and arterials at 10 Hz resolution. The macroscopic approach on the other hand uses volume, average speed and heavy vehicle percentages over a time interval, along with site properties to predict lane change intensity. This research uses macroscopic traffic and site parameters that are readily available to state DOT's for ease of implementation. The model developed in this study is applicable only for freeway segments neat interchanges and does not apply to interrupted flow facilities. Finally, the model application should be restricted to the range of variables used to calibrate it. While the model will still generate results when such variables are out of range, it will caution the user about the reliability of the reported results.

1.4 Organization of the Report

This report is organized as follows. Following this introductory chapter, Chapter 2 covers the pertinent technical literature on the topic of lane change prediction. Chapter 3 documents the field data collection sites and explains the data collection and extraction methodology using advanced video processing for capturing lane changes. Chapter 4 documents the steps used to develop the two predictive models with and without knowledge of the number of mandatory lane changes. Chapter 5 documents the combined field/simulation case study applied at the weaving segment on EB I-40 between Harrison Blvd. and Wade Avenue to test the effectiveness of a proposed treatment to mitigate discretionary lane changes. Chapter 6 describes the web-based tool developed for the model implementation. Additional documentation of the tool will be available online once the research team implements it on the ITRE server. Finally, Chapter 7 provides conclusions and recommendations for future work in this area.

CHAPTER 2 : LITERATURE REVIEW

This chapter presents a review of past studies related to freeway lane change analysis. It is divided into two major sections. The first section discusses the state-of-the-art models for predicting lane changes on freeways. In the second section, different strategies developed to limit excessive lane changing and the resulting friction are discussed.

2.1 Predicting Lane Change Frequency

Early studies on predicting lane change frequency date back to 1970 (Worrall & Bullen, 1970; Worrall, Bullen, & Gur, 1970). These studies considered drivers' lane change decision as a Markov Chain process. The authors found that the average frequency and pattern of lane changes exhibit a systematic, although weak, relationship to traffic and roadway conditions. Chang and Kao (1991) developed two models for uncongested basic freeway segments: a Poisson and a Logistic regression model, to estimate lane change rate and lane change frequency, respectively.

The ratio of speed, density, and average headway between the target and the current lane were the key independent variables of these models. However, these studies, despite being pioneers in the field of freeway operation, suffered from a lack of observation and variation of study sites. Moreover, site-specific variables like geometric characteristics were not considered in the models. These issues were resolved to a significant extent with the availability of more trajectory level data and powerful computational tools in the last few decades.

A pool of microscopic lane changing models have been developed in recent decades (Moridpour, Sarvi, & Rose, 2010; Schakel, Knoop, & van Arem, 2012; Thiemann, Treiber, & Kesting, 2008). Those models are beneficial for calibrating microsimulation models. However, the primary focus of this literature review is on macroscopic, or flow based lane changing models. Nonetheless, a few microscopic lane-changing models are described here for the sake of discussing some model development techniques.

Applications of the Markov Chain process to predict lane changes are found in several studies. Toledo et al. (2005) developed a model to predict lane change probability by incorporating target lane choice with a traditional gap acceptance model using Next Generation SIMulation (NGSIM) data on I-395, Arlington, VA (NGSIM homepage.2006). This research was later revised and improved by Toledo and Katz (2009) by incorporating a Hidden Markov Model (HMM). The motivation behind this improvisation was to capture the effect of unobserved decisions made by drivers while choosing a lane. The initial research proposed a utility model for each target lane as a function of their microscopic traffic characteristics. This utility function gives an estimate of the probability of selecting a lane as a choice lane. The critical gap for an individual was estimated as a log-normal distribution. Finally, the likelihood of a lane change is estimated by multiplying two probabilities: the probability of selecting that lane as a choice lane and probability of moving to the target lane given that a sufficient gap is available. The addition of HMM improved the target lane selection model developed in the initial research. Nonetheless, the improved model solely depends on various microscopic inputs. Singh and Li (2012) also used a Markov Chain process to predict lane change probability and estimate lane-based density in a basic freeway segment. One critical step of predicting lane changes based on this study was estimating the probabilities of changing or keeping a lane for all combinations of origin-target lanes. This study collected field data from loop detectors on two different days. A comparison between these two days of data showed that these probabilities do not change significantly. However, the long-term average of these probabilities should have been estimated from a broader range of data.

Regression models were also employed in several past studies on predicting lane change frequency on freeways. The weaving segment analysis of the Highway Capacity Manual (HCM 2016) presented two regression models for estimating lane changes per vehicle, one for weaving and another for non-weaving vehicles. These models were originally developed by Roess and Ulerio (2009) based on data collected from 14 sites across the US. The model for estimating lane changes per weaving vehicle is composed of two parts: a minimum lane change rate and an additional lane change rate. The minimum rate can be calculated from the geometry of the segment. A regression model was developed for the additional lane change rate as a function of the segment length, number of lanes, and interchange density. However, as the study recognized, the validity of the model for lane change per non-weaving vehicles is questionable. The data used in this study showed that two separate linear equations are required to model non-weaving lane change rates. This issue that presumably rose due to lack of data between 1,500 to 2,200 lane changes per hour was tackled by proposing three separate models. Although this solution prevented a discontinuity in the model, it resulted in some counterintuitive coefficients of some parameters along with a very poor fit for some sites. Nonetheless, all these models were kept in the following version of HCM (HCM6). Lee et al. (2016) proposed an exponential model to estimate the discretionary lane change rate (lane changes/vehicle/hour) using NGSIM data collected from the US-101 and I-80 site. The study noted that although the key motivation behind discretionary lane changes is the speed difference between lanes, a lot of discretionary lane changes may occur even with a negative relative speed if sufficient gaps (leader and follower) are available. Hence, it incorporated the relative gap from the lead vehicle with the relative average speed between the current and target lane in the model. The cumulative distribution of relative gap and relative velocity during discretionary lane changes showed a significant shift from that during no lane change instances. Despite generating intuitive outcomes, this model assumed that relative velocity and relative gap between the origin and target lane are independent of each other. This issue may not affect the quality of the model when the traffic speed in the dataset does not vary significantly, but an interaction term between these two parameters should be tested.

In addition to the studies discussed above, a few researchers focused on empirically analyzing the trend of lane change frequency with changing traffic characteristics. Knoop et al. (2012) analyzed the change in lane change rates (per hour-km) with lane-based density using trajectory data collected from three sites. However, some counterintuitive results led to the conclusion that the outputs are mostly site-specific. Gan and Jin (2015) estimated the total number of left-lane changes in a weaving segment using lane-based loop detector data. It showed that the number of left-lane changes increases from the leftmost lane to the rightmost lane, and that the total number of left-lane changes mostly depends on the entry flow. The outcomes of these studies might be useful for improving the operation of the selected study site, but their application for different sites necessitates a robust statistical modeling tool.

2.1.1 Summary of Past Studies: Predicting Lane Change Frequency

A summary of the review of the past studies discussed above is provided in Table 2-1, highlighting the type of model developed, variables used, and lane change and segment type focused. From the above discussion, it is apparent that the regression models proposed in HCM weaving segment analysis employed data from a wide range of sites, while models developed by other studies are mostly site-specific. Nonetheless, the HCM model generated counterintuitive coefficients for some parameters. Several studies developed well-calibrated probabilistic models to predict lane changes, but those required microscopic level data. In addition, the effect of freeway segment types on lane change frequency was not addressed by most studies.

Table 2-1: Summary of the review of lane change frequency prediction studies

Reference	Model type	Dependent variable	Independent variables	Lane change type	Segment type
Toledo et al. (2005)	Lane choice and gap acceptance model	Lane change likelihood of a vehicle	Microscopic traffic characteristics of current and target lanes	Both mandatory and discretionary	Diverge, weaving
Toledo and Katz (2009)	Lane choice, gap acceptance, and Hidden Markov model	Lane change likelihood of a vehicle	Microscopic traffic characteristics of current and target lanes	Both mandatory and discretionary	Diverge, weaving
Singh & Lee (2012)	Markov Chain	Lane-based density	Segment length and lane-based speed	Discretionary	Basic
HCM (2010, 2016)	Non-linear Regression model	Lane change/veh-hr.	Segment length, number of lanes, interchange density, weaving and non-weaving flow rate	Weaving and non-weaving lane changes	Weaving
Lee et al. (2016)	Exponential regression model	Lane change/veh-hr.	Relative velocity and relative gap between current and target lane	Discretionary	Weaving, overlap
Knoop et al. (2012)	Observational analysis	Lane changes per hr.-km	Lane-based density	Discretionary	Merge, diverge
Gan and Jin (2015)	Observational analysis	Lane changes/hr.	Lane-based flow rate	Left-lane changes	Weaving

2.2 Lane Change Control Strategies

In the vicinity of a merge, diverge, or a weave bottleneck, the impact of abrupt and excessive lane changes can be severe (Chen & Ahn, 2018; Daganzo, Laval, & Munoz, 2002; Laval & Daganzo, 2006). Therefore, several conceptual techniques have been developed to limit excess lane changes near interchanges during peak hours (Daganzo et al., 2002; Soekroella, Hegyi, Hoogendoorn, & van Kooten, 2012; Spiliopoulou, Papageorgiou, Herrera, & Muñoz, 2016; Wang, Ma, Henrickson, Wang, & Yang, 2015). It should be noted that traffic agencies use solid white stripe to restrict lane changes permanently near ramp gore areas and work zones (FHWA, 2009) . This literature review mostly focused on real-time implementation techniques of controlling lane changes at freeway weaving and diverge segments.

2.2.1 Weaving Segment

Daganzo (2002) proposed a modified ramp metering technique to reduce the friction induced by the lane changing maneuvers of ramp entering vehicles in a weaving segment with a two-lane entry ramp (Figure A-1 (a)). According to this technique, vehicles going from ramp to ramp (green line) must position themselves on the rightmost lane which is unsignalized. Vehicles going from ramp to freeway (red line) will be on the second from the right lane facing a signal. Thus, a portion of the entry ramp traffic can travel without any restriction, and exiting traffic coming from the freeway faces less restriction while performing the weaving maneuver.

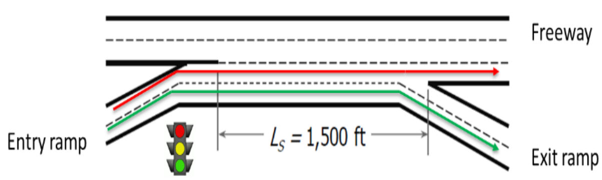

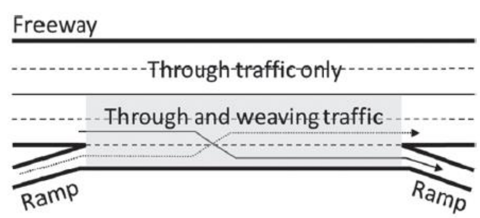

Figure 2-1: (a) Reducing lane change induced friction by a modified version of ramp metering (Daganzo 2002) (b) Dynamic lane assignment in weaving segment (Wang et al. 2015)

Wang et al. (2015) proposed to divide a freeway weaving segment laterally to minimize the impact of mandatory lane changes on non-weaving vehicles as shown in Figure A-1 (b). Here, the leftmost lane(s) are assigned to a major portion of freeway through traffic only. The rests are assigned to the remaining rightmost lane(s). The shaded area is analyzed as a weaving segment, while the remaining leftmost lanes can be considered as a basic freeway segment. The number of lanes assigned to each sub-segment is estimated by maximizing the total throughput while maintaining sufficient capacity for the subsegments. Zhao et al. (2016) adopted this dynamic lane assignment technique of Wang et al. and combined a ramp metering strategy with it. It developed a multi-objective optimization tool to minimize the complexity of the treatment and maximize the throughput. Both Wang et al. and Zhao et al. implemented HCM-based models in their optimization algorithm.

2.2.2 Diverge Segment

Daganzo (2002) proposed that banning lane changes near an exit ramp can prevent the capacity drop during congested conditions. As shown in Figure 2-2, lane changing is prohibited for the two rightmost lanes near the exit (indicated by solid lines). Upstream of the queue (at the start of the solid line), vehicles that need to take the exit are encouraged to change lane.

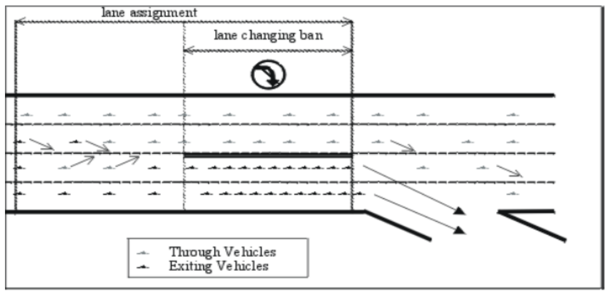

Figure 2-2: Lane change control strategy at a diverge segment

Soekroella et al. (2012) adopted the concept of Daganzo (2002) to mitigate queue spilling back to an off-ramp from a surface street bottleneck by segregating exiting and through traffic. The contributions of the study are that it quantified the impact of such segregating treatment and that it developed two automated controlling schemes to optimize the length of the lane change ban upstream of the exit ramp gore. A few more studies assessed the impact of lane changes near freeway diverge segments using traffic flow theory, but those did not focus on mitigation strategies (Jin, 2010; Chen and Ahn, 2018).

2.2.3 Summary of Past Studies: Lane Change Control Strategies

It is apparent from the above discussion that only a few techniques to control lane changes were developed by past research for freeway weaving and diverge segment. To the best of our knowledge, no technique has been developed to control lane changes for merge segments and for within interchange areas. In addition, the benefits of these techniques need to be assessed by simulation. The feasibility of implementing these strategies also needs to be considered in future research.

CHAPTER 3 : DATA COLLECTION AND EXTRACTION FOR PREDICTIVE MODEL DEVELOPMENT

This chapter describes the data collection effort carried out by the research team for developing the predictive model for lane changing frequency. Note that field data were also required to assess a treatment strategy, which Chapter 5 of this report describes. However, within the radius in which a field survey is feasible for the research team, no treatment had been implemented during the project timeline. Hence, a simulation study was carried out (see Chapter 5) and its data collection requirements were different than that for the model development task. Therefore, that data collection effort is described separately in Chapter 5.

This chapter begins with a discussion of the site selection criteria and a short description of the selected sites. Then, it describes the video data extraction method adopted in this study. Following that, it explains the structure of the fused database along with the definitions of the model parameters. The key points are summarized in the last section.

3.1 Identify Data Collection Sites

The choice of a data collection site for any research purpose is strongly governed by what data elements must be observed. For developing a macroscopic or analytical lane change prediction model, important data elements include road geometric and aggregated traffic characteristics data such as lane change frequency, flow rate by vehicle class and origin-destination routes, average speed, and average density. Details about these data elements are described later in this chapter. Based on these required data elements, the research team defined a set of criteria for selecting each data collection site. The following subsection discusses the site selection criteria, followed by the final list of data collection sites.

3.1.1 Site Selection Criteria

Good Visibility of Segment Boundaries: The boundaries of weave, diverge, or merge segments are often defined by the location of the ramp junctions. For example, in a weaving segment, it is crucial to collect the vehicle count by their origin-destination routes. Hence, it is recommended that the entry and exit gore points of a weave must be covered when collecting traffic data from a site. This condition restricts the choice of data collection sites due to the coverage capacity of the data collection tool used.

Among different traffic data collection devices, video camera is the most accurate means for collecting lane change data of all vehicles in a traffic stream. Both ground and drone cameras were available to the research team for this project. Ground cameras cover only up to 300 ft. stretch of a straight road given that it is placed on an overhead bridge or gantry. Hence, the use of this type of camera requires the site to be short and to have a suitable location to install the camera. This sort of camera, however, is advantageous in the sense that it can record for multiple days because of their low power consumption rate. To cover a relatively long site, high-resolution cameras mounted on a drone are more appropriate. However, their application is limited due to their short battery life and because of federal regulations about the proximity of the site to any air traffic route. The research team weighed all these constraints for selecting a data collection site and choosing the most appropriate fashion to survey that site.

Geometric Diversity: To develop the predictive model, it is imperative to have data from sites covering a wide range of geometric characteristics. Geometric characteristics that tend to influence lane change frequency of an IIA include the segment type, e.g., weaving, diverge, merge, and basic (see HCM6 for definitions), segment length, number of lanes, nearest ramp locations, and lane change requirement for merging and diverging vehicles. The research team leveraged different mapping tools to understand the geometric characteristics of potential sites so that the final list of sites has significant geometric variability.

Traffic Variability: While it was difficult to understand the detailed traffic characteristics of a site before collecting the data, the research team leveraged the available AADT data (NCDOT, 2018) and Google Map's live traffic feature (Google, n.d.) to characterize traffic characteristics of a site at different times of a day. The location and times of data collection were selected in such a way that the traffic flow rate and speed varied over a wide range.

Geometric Homogeneity within Sites: It is desirable that within the coverage area, each selected site is homogeneous in terms of its geometric properties, e.g., segment type, number of lanes, curvature, and grade.

3.1.2 List of Data Collection Sites

Weighing the abovementioned criteria, the research team selected 16 data collection sites. Table 3-1 presents a list of these sites along with their segment type, duration of video records, and camera type used for each site. Note that the data from US-101 in Los Angeles, CA (Site 14,15, and 16) were collected and made available through the Next Generation Simulation data collection effort taken by FHWA in 2005 (NGSIM homepage, 2006). Also, the data from I-440 EB at Western Blvd. (Site 1) were primarily used for general exploration of lane change and other traffic characteristics. We did not use these data in the model development task because of the low resolution of the video.

Table 3-1: List of data collection sites

Site No.	Site	Duration (min)	HCM6 Segment Type	Camera Used
1	I-440 EB at Western Blvd (Pilot)	895	Upstream of Merge	Ground
2	I-440 EB at Ridge Rd	475	Weave	Ground
3	I-40 WB at Wade Ave. (facing east from Trenton Rd. bridge)	50	Downstream of Merge	Ground
4	I-40 WB at WadeAve. (facing east from Trenton Rd. bridge)	55	Downstream of Merge	Ground
5	I-40 EB at S. Saunders St and Hammond Rd	85	Weave	Drone
6	I-40 WB at S. Saunders St and Hammond Rd	85	Weave	Drone
7	I-440 EB at Poole Rd and US-64	35	Weave	Drone
8	I-440 WB at Poole Rd and US-64	30	Weave	Drone
9	Wade Ave. WB at Blue Ridge & I-440	125	Weave	Drone
10	I-440 EB at Hillsborough St Exit	90	Diverge	Drone
11	I-40 EB at I-440 (MM 293)	35	Basic	Drone
12	I-40 WB at I-440 (MM 293)	35	Basic	Drone
13	I-40 EB at I-440 (MM 309)	40	Basic	Drone
14	US-101 in Los Angeles, CA (Weave)	40	Weave	Ground
15	Upstream of US-101 in Los Angeles, CA	40	Basic	Ground
16	Downstream of US-101 in Los Angeles, CA	40	Basic	Ground

3.2 Generate the Fused Database

Following the collection of the video records, the next task was to convert the necessary data from these into digital formats. Thus, traffic data were fused with site inventory data. We collected the site inventory data – i.e., segment length, number of lanes, minimum lane change requirements, and nearest ramp locations for these sites using Google Earth and Google Maps. The following subsection describes the various video data extraction methods that the research team explored.

3.2.1 Video Data Extraction Methods

The most challenging aspect of using video records to collect traffic data is to convert the data into digital formats for subsequent analysis. In this regard, the research team investigated the use of several techniques. For simple traffic counts, manually counting the entering vehicles from the videos is the most straightforward way. However, in addition to traffic counts, the research team needed to estimate the average speed, number of lane changes, count by vehicle class, and by origin-destination route. Hence, the research team could not rely solely on manual counting and sought automated video data extraction methods. Below are some data extraction tools that the research team explored.

- An open-source tool for lane change detection: Sala et al. (2020) developed a semi-automated tool to detect lane changes from videos captured from ground cameras. The research team successfully used this tool for several sites, but the outcome was not satisfactory for drone videos and videos that had shadow effects.
- Goodvision: Goodvision (n.d.) is a web-based service that can analyze different kinds of traffic videos. The process of estimating traffic flow rates by vehicle class and origin-destination route, lane change frequency, and average speed is faster than manual counting using this tool. It allows the user to draw on the video frame a line-shaped feature called "traffic gate". Traffic gates generate the records of how many vehicles cross it and the corresponding timestamp. However, this tool was deemed to be not sufficiently accurate with videos captured from drones.
- DataFromSky: DataFromSky (n.d.) is also a web-based service to analyze traffic videos captured from drones. Its video processing speed is a bit slower than that of Goodvision, but still significantly faster than that of manual counting. In addition, it has a video stabilization feature which is very convenient for extracting data from drone videos. This tool also has the "traffic gate" feature. The most potent feature of this tool is that the user can generate vehicle trajectory data– either in pixel unit or in geographic coordinates, but to extract real world trajectories is an expensive proposition. One drawback of this tool is that it cannot reliably track heavy vehicles, although it distinguished heavy vehicles from passenger cars with sufficient accuracy.

After exploring all these options, the research team decided to employ different techniques as listed below –accounting for their strengths, weaknesses, and suitability for different sites.

- Due to the low-resolution of the camera used at I-440 EB at Ridge Rd., traffic data from it were extracted manually. This was possible because the segment length is only 275 ft.
- The research team used ground cameras to collect data from Interstate 40 westbound at Wade Ave. (Site 3 and 4) because there was an overhead bridge. We purchased the service of Goodvision to extract data from these videos as this tool showed satisfactory performance with videos captured by ground cameras. The outputs were verified by manually cross-checking 10% of the estimated vehicle counts and lane changes.
- For the remaining sites (from Site 5 to 13) where the video was captured from a drone, the research team purchased the service of DataFromSky (DFS) because of their video stabilization feature and sufficient accuracy with extracting data from drone videos. The process was supplemented by a rigorous manual verification. However, the heavy vehicle lane changes were counted manually, for this tool could not track those very well.

It is necessary to explain the steps of extracting traffic data using automated tools so that the level of effort required beyond the third party digitization is well documented. The main step, which is estimating lane change frequency, flow rate, and average speed using traffic gates, is identical for both DataFromSky and GoodVision. Because the former one was used for most sites, its in-and-out processing steps are summarized below.

3.2.1.1 Steps to Extract Traffic Data from Videos using DFS Tool

Step 1 – Upload Video for initial processing: Frist, the **user** uploads the drone video to the DFS website.
Step 2 – Generate a 5-minute processed sample video: Next, the **vendor** processes the first 5-minute of the video at no cost so that the user can check the accuracy before ordering the full video process. The processed video can be opened using offline software developed by vendor
Step 3 – Check sample and order full processed video: The **user** checks using the offline software if vehicles are properly tracked and the frame is stabilized in the 5-minute video. Once assured, the user requests the full processed video either in pixel units (less expensive) or in geographic units (more expensive).
Step 4 – Generate full processed video: The **vendor** generates the full processed video at the pre-specified cost[1].
Step 5 – Extract traffic and lane change counts and speed: The **user** employs the functionality of the offline software to estimate traffic flow rate, lane change count, and speed. A feature called traffic gate is drawn on the video frame using the software as shown by the colored lines in Figure 3-1. The software then generates the gate crossing event dataset in a .csv format. Each row of the output dataset represents a crossing event. The columns are: a) a unique vehicle ID for each crossing vehicle, b) the gate ID being crossed, c) timestamp of the crossing event, and d) vehicle class (e.g., passenger car, truck, or bus). The technique of estimating different traffic information using this software is explained below.

i. Traffic entry flow rate (vehicles per hour): Figure 3-1 shows the application of traffic gates for estimating traffic flow rate for the direction shown by the black arrow. The purple gates are created to estimate the entry flow rate. Because the tool also classifies vehicles, flow rate by vehicle class is also obtained in this way. A separate entry gate is created for each lane so that the entry lane ID for each entering vehicle is recorded. Entry lane ID for each vehicle is important for estimating traffic flow rate by origin-destination routes and for identifying the direction of a lane change in the later steps.
ii. Lane change count (per hour): The green gates in Figure 3-1 are drawn along the lane marking to capture the lane changing events. The direction of each lane change is determined by fusing the entry lane data for the corresponding vehicle obtained in the previous step. For example, the trajectory shown by the dashed green line crossed the lane marking between lane 5 and lane 4 (lane 5 is the rightmost lane). Since it is known from the purple gate crossing event that this vehicle entered through lane 5, it can be ascertained that the crossing of the lane marking was due to a lane change from lane 5 to lane 4.

[1] Details about the cost structure is listed here https://drive.google.com/file/d/1TGywQh8PkB1SQcGYFTf8b68BM-V_XlPz/view

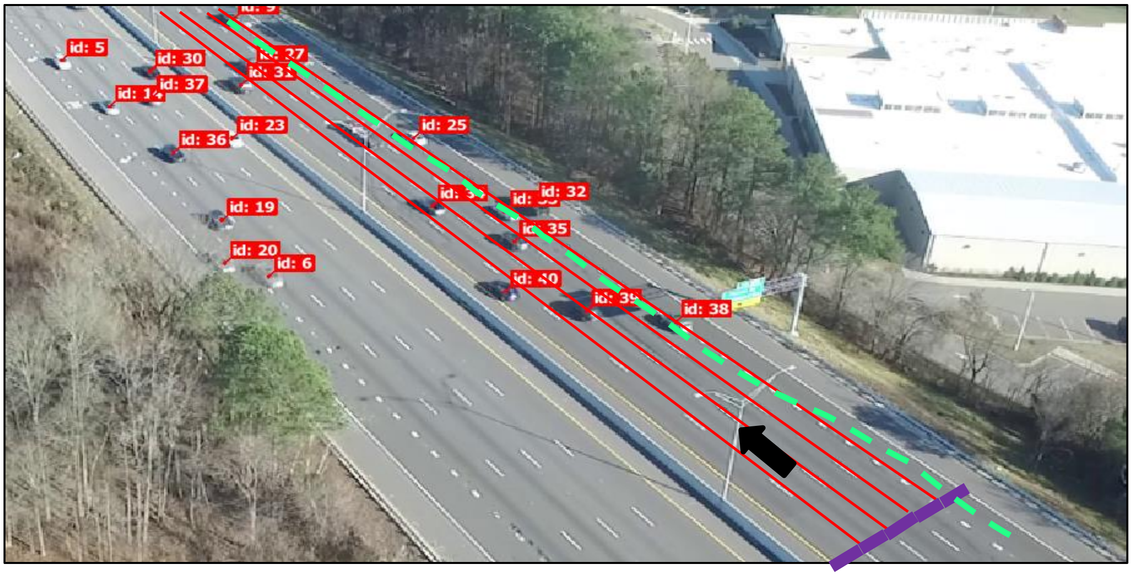

Figure 3-1: Traffic gates drawn using the DataFromSky software to estimate flow rate and lane change frequency

iii. Traffic flow rate by origin-destination route (vehicles per hour): As explained above, the purple gates give the entry lane ID, and the green gates give the lane change information. Combining these and updating a vehicle's lane position after each consecutive lane change, we get the exiting lane ID of the vehicle. Thus, the origin-destination route for each vehicle is easily determined from the lane configuration of the site.

iv. Space Mean Speed (SMS) (miles per hour): The first step to estimate the Space Mean Speed (SMS) of the traffic stream is to create traffic gates at two points between which the geographic distance is known. For instance, in Figure 3-2, the two red gates are drawn at the foot of the two lampposts because the locations and the distance (l) between these two posts can be easily obtained from Google Earth or Google Map's satellite imagery. From the time difference of the crossing events of these two gates for each vehicle (Δt_i), SMS at a period *t* is estimated using equation 3-1.

$$SMS_t = \frac{n_t l}{\sum_{i=1}^{n_t} \Delta t_i} \qquad \text{Eq. 3-1}$$

Where i = 1,2,3…. n represents vehicle ID. n is the total number of vehicles entered into the segment within time interval *t*.

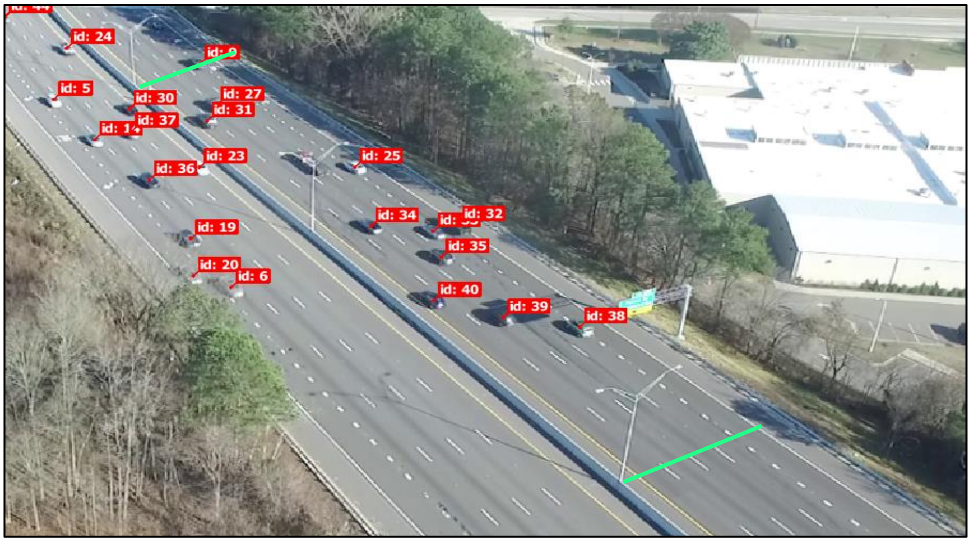

Figure 3-2: Traffic gates drawn using the DFS software to estimate Space Mean Speed

v. Average Traffic Density (vehicles per mile per lane): Average traffic density in any time period t (k_t) is estimated by entering the SMS and flow rate into the fundamental equation of traffic flow as shown in equation 3-2.

$$k_t = flow\ rate_t / (Number\ of\ lanes * SMS_t) \qquad \text{Eq. 3-2}$$

<u>Step 6 – Manual Verification</u>: The entry lane ID for 10% of all vehicles and lane changes for 10% of the passenger cars in a video were manually checked to ensure that the performance of the tool is satisfactory. It was found that if the gates are positioned appropriately so that the parallax error is counterbalanced, the error rate for the entry lane ID was close to zero, while that for passenger car lane change count was about 5%. Heavy vehicle lane changes, as mentioned earlier, were tracked manually.

3.3 Structure of the Database

Fusing data from all the sites, the research team constructed a fused database to be used in the model development process. The database contained data from a total of 15 sites (excluding the pilot site). The number of observations per site ranged from 6 to 95. To predict the total lane change frequency per hour, all important predictor variables are organized in appropriate units in the database. All data elements were aggregated in 5 minutes interval. The full database, as provided in Appendix A of this report, contains 33 predictor variables and 247 observations. Below is the description of the predictor variables that were finally incorporated into the predictive model.

3.3.1 Site Geometric Properties

There are five segment geometric properties in the database as described below. The value for these parameters is fixed for each site. Figure 3-3 explains these properties with examples of a weave and a diverge segment. The sites of interest are marked by green rectangles in this figure.

Segment Length (ft.): Segment length is an important factor for predicting total lane change frequency because the optional lane changes by a vehicle tend to increase with the distance traveled. As mentioned earlier, it is recommended to include the governing ramp-junctions within the segment length such as on-ramp gore for merging, off-ramp gore for diverging, and both ramp gores for weaving segments.

Number of Lanes: A higher number of lanes in a segment means more lateral space to change lanes compared to a narrower segment. The traffic density estimated using equation 3-3 also requires this variable as an input. It is defined as the total number of lanes at the site, including any auxiliary, acceleration, or deceleration lanes.

Minimum Lane Changes for Entering/Exiting Vehicles: That variable is defined as the minimum number of lane changes an entering or exiting vehicle through ramp junction must make. It is denoted by LC_{FR} for exiting and by LC_{RF} for entering vehicles, following the weaving analysis convention in HCM6. These variables were directly input in the modeling process and also used to estimate another input variable called the total minimum lane change frequency. As shown in Figure 3-3, each ramp-to-freeway vehicle must make at least two lane changes to get on to the freeway ($LC_{RF} = 2$). On the other hand, a freeway-to-ramp vehicle does not have to change lane ($LC_{FR} = 0$) if it positions itself on lane 4 prior to entering the site.

Nearby Ramp Position and Distance (ft.): The distance to the closest on-ramp and off-ramp is another potential influential factor for estimating the lane change frequency. Their effect is different depending on the type of the ramp (e.g., on-ramp or off-ramp) and their position relative to the study area. In this study, the distances to the closest on-ramp and off-ramp are measured from the center of the site to the gore point of the corresponding ramp. If the closest ramp is located upstream of the center of the site, the measured distance is reported as a negative number. If the closest ramp is located downstream of the center of the site, the measured distance is reported as a positive number. Figure 3-3 shows examples of the signed distances to the closest ramps.

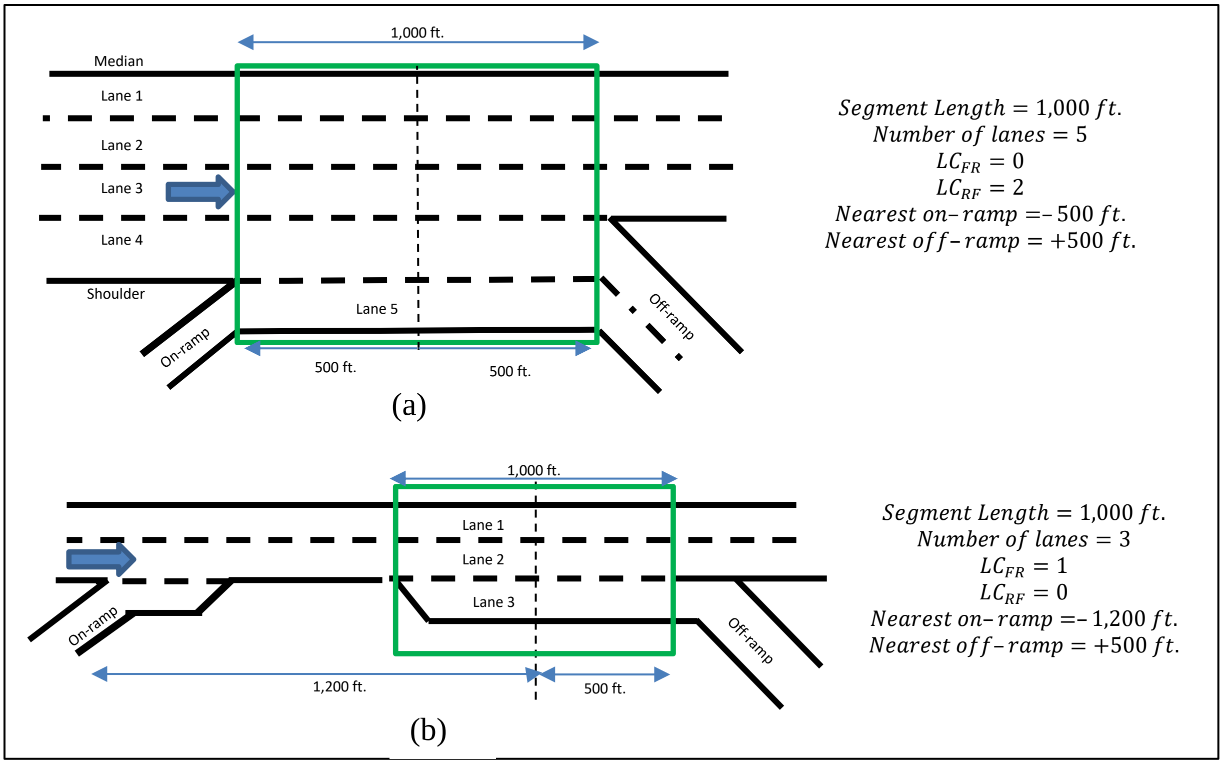

Figure 3-3: Examples of site characteristic parameters (a) for a weave (b) for a diverge segment

3.3.2 Traffic Characteristics

Traffic characteristic parameters change with every time aggregation interval. In addition to the response variable, which is the total lane change frequency, there are six traffic parameters selected in the final lane change prediction model as described below. Among these, flow rate, space mean speed, and average traffic density have already been described in section 3.2.1.1. Flow rate (in vehicles per hour) for passenger cars and heavy vehicles are estimated and used as separate variables. The total flow rate is divided by the total number of lanes to get the total flow rate per lane (vehicles per hour per lane). Space mean speed and average traffic density calculations are explained in Eq. 3-1 and Eq. 3-2, respectively. The remaining traffic variables are described below.

Minimum Lane Change Frequency (per hour): The minimum lane change frequency (MinLaneChanges) observed within a time interval depends on the freeway-to-ramp and ramp-to-freeway flow rates as well as on the two site characteristic parameters, LC_{FR} and LC_{RF}, as described above. It is estimated as shown in equation 3-3. It is important not only because it is a fraction of the total lane change frequency but also because these lane changes may trigger more discretionary lane changes.

$$MLC\ per\ hour = v_{FR} * LC_{FR} + v_{RF} * LC_{RF} \qquad \text{Eq. 3-3}$$

Where v_{FR} and v_{RF} are the flow rates (vehicles per hour) on the freeway-to-ramp and ramp-to-freeway routes, respectively. All other parameters have been explained earlier. Note that for merge segments, both v_{FR} and LC_{FR} are always zero. Likewise, both v_{RF} and LC_{RF} are always zero for diverge segments.

Vehicles-Miles Traveled: It is estimated as the product of the length of the segment (miles) and the total flow rate (vehicles per hour). It measures the amount of travel for all vehicles in a site for a given period, which is expected to have an increasing effect on the total lane change frequency.

3.4 Summary

This chapter covered all aspects related to the data collection and extraction effort, including the site selection criteria, list of sites, data extraction techniques, and description of the fused database. The research team spent a significant effort on this task, for the quality of the predictive model directly depends on the quality of the input data. Each of the selected sites have unique geometric characteristics. Hence, the research team needed to improvise the data collection and extraction method for each location based on their judgment and experience. The full database is attached in Appendix A of this report.

CHAPTER 4 : PREDICTIVE MODELS

This section presents the methodological details and results regarding the predictive models for lane change frequency. It begins with identifying the possible data sources for the predictor variables of the model because these data must be collected or estimated in an appropriate fashion for applying the model. Then the model development and testing procedures are explained. Following that, the modeling results are presented. Finally, the performance measures and limitations of the model are described.

4.1 Possible Data Sources for Predictor Variables

In the previous chapter, the predictor variables that were finally included in the model were introduced. This section suggests for these variables the possible data sources based on current practice in transportation engineering. Table 4-1 summarizes the list of possible data sources, divided into two categories: from field measurements and from existing models

Table 4-1: Possible data sources for the required predictor variables in the model

Required Variables	Possible Data Source(s)	
	Field measurement tools	**Existing sources / models**
All geometric data	Mapping tools, road inventory, aerial photos	-
Flow rate by vehicle class	Traffic monitoring cameras, roadside sensors, loop detectors.	AADT adjusted hourly volumes for passenger cars & heavy vehicles
Space Mean Speed	Probe database, roadside sensors, loop detectors, traffic cameras	Highway Capacity Manual (TRB, 2016) models for different segment types*
Average traffic density	Roadside sensors, loop detectors, traffic cameras	Fundamental equation of traffic flow (Eq. 3-2)
Freeway-to-ramp and Ramp-to-freeway flow rate	Traffic cameras, traffic counters at on-ramp (for merge) or at off-ramp (for diverge), Bluetooth sensors, license plate matching surveys.	Using freeway and ramp entering and exiting traffic counts and assuming either maximum weave** or average weave***

**Explained in detail in Appendix B*

**A*ssumes all vehicles entering through the on-ramp merge and all entering through the freeway exit*

****Assumes that the exit ramp draws the same proportion of traffic from the freeway and the on-ramp. Explained in detail in Appendix B.*

4.2 Modeling Approach

The statistical methodology used to create the predictive models for hourly lane changes is known as partition models, recursive portioning, and classification and regression trees. The seminal reference is the 1984 book by Leo Breiman (Breiman et al., 1984).[2] The implementation used was the "rpart" package of the R software environment for statistical computing and graphics.[3]

As compared to linear regression and related techniques, partition models can more readily handle both categorical and numerical variables as predictors, nonlinear relationships between predictors and the response, and interactions between and among predictors. The only modeling decision is the choice of a "complexity" parameter that controls that number of terminal nodes, also called leaves, in the final tree. This choice is the canonical one between "model fit" and complexity.

The trees employed by the Lane Change Prediction Tool (LCPT) have Total (Hourly) Lane Changes as the response, and candidate predictors that are a combination of user inputs and variables derived from inputs within the LCPT. Section 3.3 presented the definitions for these variables. Table 4-2 lists the candidate predictor variables. Not all of them appear in the final trees.

[2] A brief summary is available from Wikipedia, at https://en.wikipedia.org/wiki/Recursive_partitioning.
[3] See https://www.r-project.org/.

Table 4-2: Input variables to the LCPT partition models

Predictor Variable	Unit	Symbol	Input or Derived?	Comment
Minimum lane change frequency	Frequency per hour	MinLane Changes	Input	Present in one model, not present in the other (when Minimum Lane Changes = xxx). Defined in Eq. 3-3
Passenger car flow rate	Vehicles per hour	PCFlow	Input	$Total\ Flow\ *\ (1 - [.01 * Heavy\ Vehicle\ Percentage])$
Heavy vehicle flow rate	Vehicles per hour	HVFlow	Input	Use this equation if only total flow and heavy vehicle % are known: $Total\ Flow\ *\ [.01 * Heavy\ Vehicle\ Percentage]$
Total flow rate per lane	Vehicles per hour per lane	TotalFlow PerLane	Derived	$Total\ Flow\ /\ Lanes$
Space Mean Speed	Miles per hour	Speed	Input	See Eq. 3-1
Average traffic density	Vehicles per mile per lane	Density	Derived	See Eq. 3-2
Number of lanes	-	Lanes	Input	-
Vehicles Miles Traveled	Vehicles-miles per hour	VMT	Derived	-
Segment length	Feet	Length	Input	-
Distance to the nearest On-ramp	Feet	OnRamp Distance	Input	-
Distance to the nearest Off-ramp	Feet	OffRamp Distance	Input	-

The LCPT contains two partition models. The first includes as a predictor MinLaneChanges, the minimum number of lane changes per hour estimated as shown in equation 3-3.

Recognizing that MinLaneChanges may not always be measured, or that the v_{RF} or v_{RF} may not be available, the second partition model does not include MinLaneChanges as a predictor. Both trees were built using a dataset containing 247 data points from 15 sites, each representing measurements aggregated over a five-minute period. Details of the data collections performed by ITRE appear in Chapter 3.

Each tree consists of a series of binary splits of a subset of the data on the basis of a single variable. To illustrate, Figure 4-1 shows the first split the tree that includes MLC. (The full tree appears in Figure 4-3). The value (1373) within the root (uppermost) node is the mean of Total Lane Changes for the root node of the tree (i.e., the entire dataset); the values below the node are the associated number of data points and the percentage of the dataset. The first split is on the value of MinLaneChanges: the 76 data points with MinLaneChanges < 450 go to the left, and the remaining 171 data points to the right. The associated means of Total Lane Changes in these two subsets of the data are 400 and 1806, respectively—a substantial difference. All further branches are analogous.

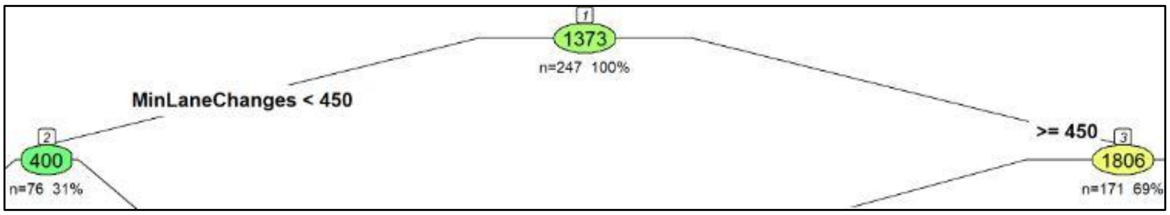

Figure 4-1: The first split in the tree in Figure 4-3.

Splits are made in order of decreasing statistical significance, which can be interpreted heuristically as sequentially the difference of the means in the two child nodes.[4] Splitting ceases when the complexity parameter, which *decreases* as the number of nodes increases, falls below a model-determined threshold calculated by means of 10-fold cross-validation, in which randomly selected subsets of the data are omitted, and the model regenerated. This process is algorithmic, and therefore fully reproducible. Figure 4-2 shows graphically the process for the tree that includes MinLaneChanges. The number of nodes is on the upper x-axis and the (relative) cross-validation error on the y-axis. The threshold is the dotted horizontal line, below which the error first falls when the number of nodes is 22. There is also the restriction that no split can create a node containing only one data point. (The only other widely employed criterion for selecting the complexity parameter is minimization of the relative cross-validation error. In general, and especially for datasets of the size we have, this leads to overfitting of the data.)

[4] Taking associated variances into account.

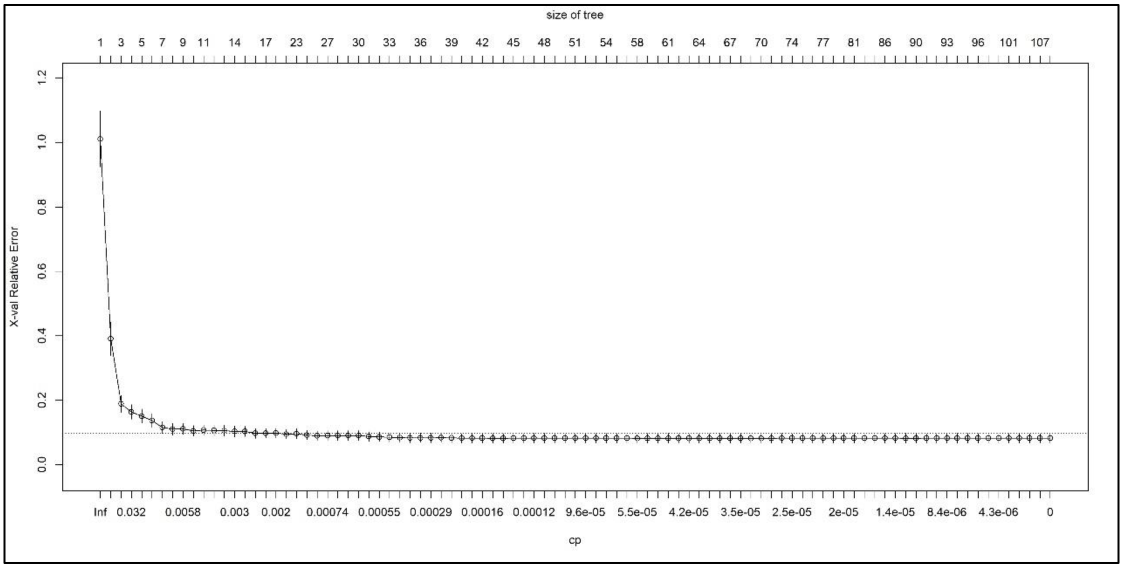

Figure 4-2: Graphical illustration of the selection of the complexity parameter for the model that includes MinLaneChanges.

To calculate the predicted value of Total Lane Changes from user inputs, the LCPT simply "drops" it through one of the two trees, and the predicted value is the mean associated with the terminal node into which it falls. The approximate standard error is the standard deviation within that node, and the confidence bounds are the mean ± the approximate standard error.

4.3 Modeling Results

Figure 4-3 shows the final partition tree used by the LCPT when a value of Minimum Lane Changes is available, either from direct measurement or using the spreadsheet calculator that accompanies the LCPT software tool. Ultimately, the model places each of the 247 data points in one of the 22 *terminal nodes*. To remind, at the root and each intermediate node, the underlying dataset, or the subset reaching that node, undergoes a binary split on the basis of one predictor variable, with splits made in order of decreasing statistical significance. The mean numbers of Total Lane Changes over the 22 terminal nodes range from 251 to 3798, and they correspond to the colors in Figure 4-3.

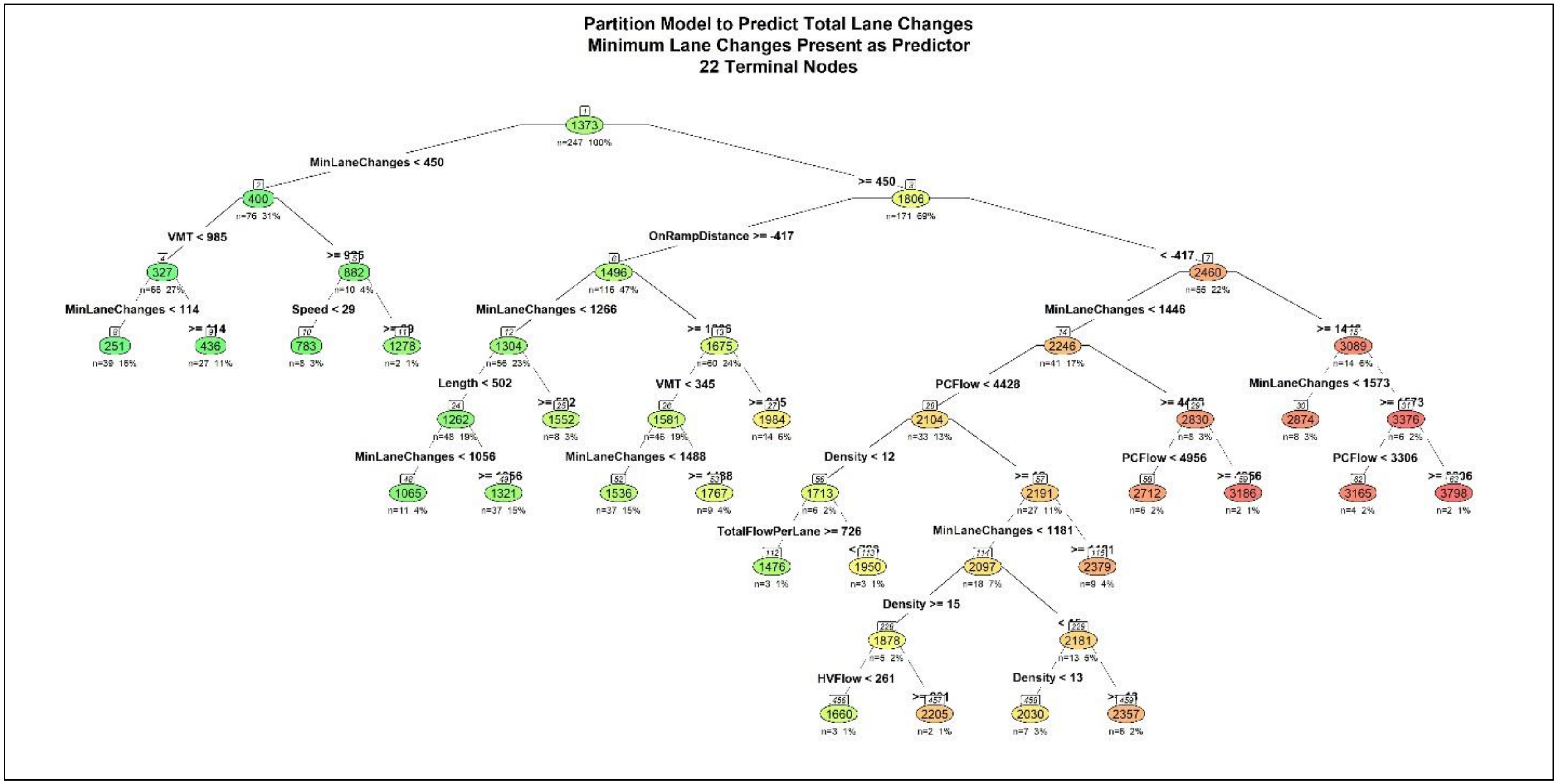

Figure 4-3: Partition model employed by the LCPT to predict Total Lane Changes when a value of Minimum Lane Changes is available

Table 4-3 summarizes characteristics of Total Lane Changes for the 22 terminal nodes in the tree in Figure 4-3. The node numbers may seem obscure but can be interpreted in the following manner. Starting for the top, each "tier" in the tree in Figure 4-3 contains nodes whose numbers begin with a power of 2 and continue to the next-smallest power of 2, minus one. To illustrate, the top tier contains only node number 1, the second tier contains nodes 2 and 3, the third contains nodes 4, 5, 6 and 7, and so on. The lowermost tier contains nodes 256, …, 511. But, because of the realized sequence of splits and the selection of the complexity parameter, not all nodes are present in the tree. So, for instance, the four leftmost terminal nodes in Figure 4-3 are 8, 9, 10 and 11, and the four at the bottom are 456, 457, 458 and 459. As already noted, when the LCPT "drops" a case through the tree, the predicted number of hourly lane changes is the mean associated with terminal node into which it falls.

Table 4-3: Characteristics of the 22 terminal nodes in the tree that includes Minimum Lane Changes as a predictor of Total Lane Changes.

Node	Count	Mean	Standard Deviation
8	39	251.08	84.20
9	27	436.44	102.86
10	8	783.00	145.81
11	2	1278.00	59.40
25	8	1551.75	159.74
27	14	1983.66	135.15
30	8	2873.82	282.26
48	11	1064.73	102.26
49	37	1321.30	73.64
52	37	1536.32	80.57
53	9	1766.67	71.44
58	6	2712.00	254.78
59	2	3186.00	449.72
62	4	3165.00	110.15
63	2	3798.00	466.69
112	3	1476.00	247.97
113	3	1950.00	222.97
115	9	2378.67	125.11
456	3	1660.00	252.95
457	2	2205.00	63.64
458	7	2030.14	114.56
459	6	2357.11	129.90

Table 4-4 summarizes how the 15 sites (rows) are distributed across the 22 terminal nodes (columns). Figure 4-4 shows that tree for the model when MinLaneChanges are *not* available. With only 11 terminal nodes it provided significantly less discrimination than the tree in Figure 4-4.

Table 4-4: Cross-tabulation of sites and terminal nodes for the tree that includes Minimum Lane Changes as a predictor of Total Lane Changes.

Site	Terminal Node																					
	8	9	10	11	25	27	30	48	49	52	53	58	59	62	63	112	113	115	456	457	458	459	Sum
I-40 S Saunders E	4	5	3	1	4	0	0	0	0	0	0	0	0	0	0	0	0	0	0	0	0	0	17
I-40 S Saunders W	1	0	5	1	0	0	0	4	5	1	0	0	0	0	0	0	0	0	0	0	0	0	17
I-40/440 Basic EB	0	0	0	0	0	0	0	1	3	3	0	0	0	0	0	0	0	0	0	0	0	0	7
I-40/440 Basic WB	0	0	0	0	0	0	0	1	2	3	1	0	0	0	0	0	0	0	0	0	0	0	7
I-40/440 East Split	0	0	0	0	0	0	0	0	3	3	2	0	0	0	0	0	0	0	0	0	0	0	8
I-40WB Weave_E	0	0	0	0	0	0	0	3	2	5	0	0	0	0	0	0	0	0	0	0	0	0	10
I-40WB Weave_W	0	0	0	0	0	0	0	1	6	2	2	0	0	0	0	0	0	0	0	0	0	0	11
I-440 at Poole Rd E	0	0	0	0	0	0	0	0	2	5	0	0	0	0	0	0	0	0	0	0	0	0	7
I-440 at Poole Rd W	0	0	0	0	0	0	0	0	3	3	0	0	0	0	0	0	0	0	0	0	0	0	6
I-440 EB at Hillsborough Ext.	0	0	0	0	0	1	0	0	6	5	1	0	0	0	0	0	0	0	0	0	0	0	13
Ridge Rd	13	8	0	0	4	13	7	1	5	7	3	6	2	0	1	3	3	3	3	2	6	5	95
US101_Dnstrm	0	0	0	0	0	0	1	0	0	0	0	0	0	4	1	0	0	1	0	0	1	0	8
US101_Upstrm	2	0	0	0	0	0	0	0	0	0	0	0	0	0	0	0	0	5	0	0	0	1	8
US101_Wve	7	1	0	0	0	0	0	0	0	0	0	0	0	0	0	0	0	0	0	0	0	0	8
Wade WB at 440	12	13	0	0	0	0	0	0	0	0	0	0	0	0	0	0	0	0	0	0	0	0	25
Sum	39	27	8	2	8	14	8	11	37	37	9	6	2	4	2	3	3	9	3	2	7	6	247

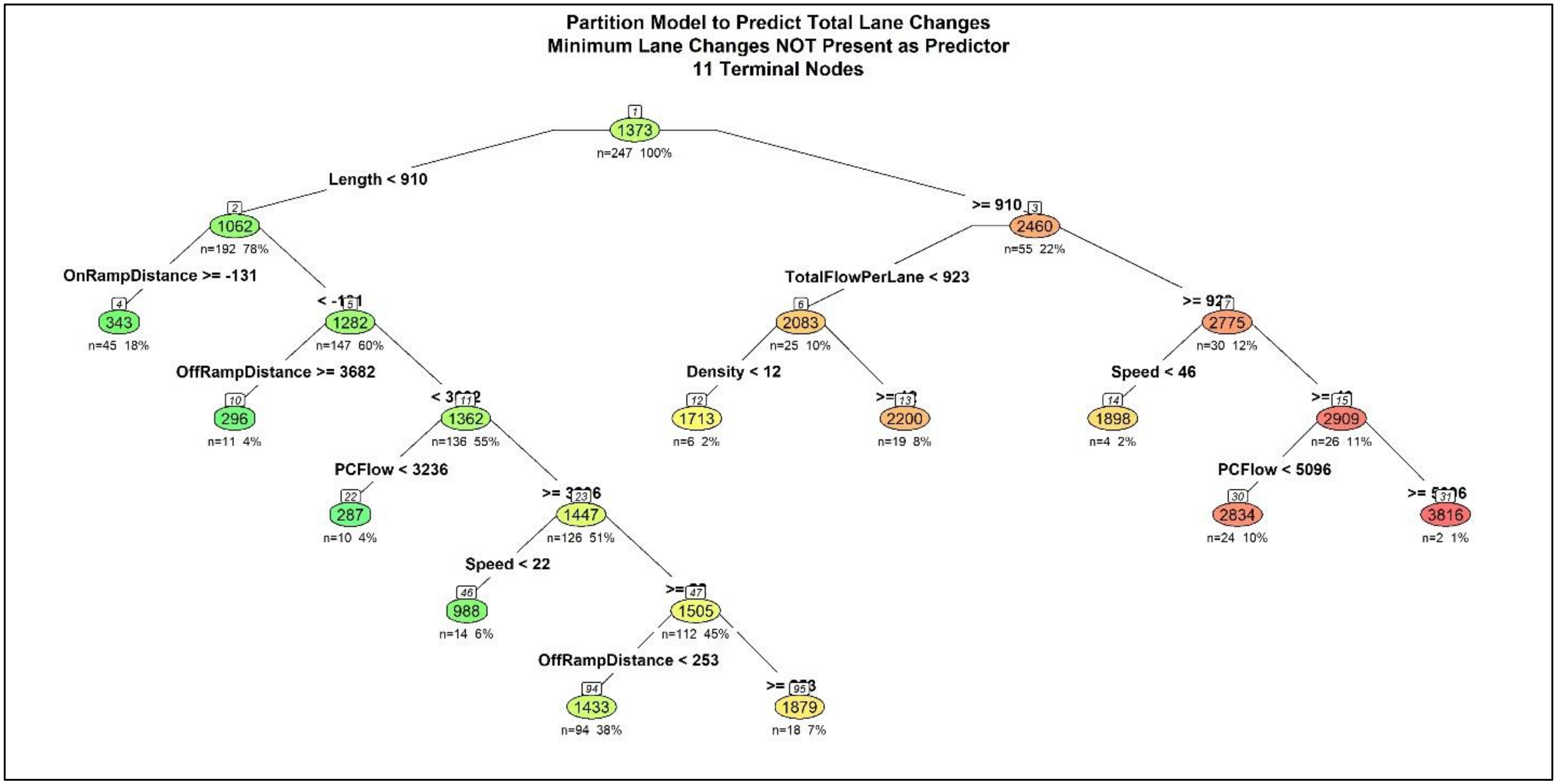

Figure 4-4: Partition model employed by the LCPT to predict Total Lane Changes when a value of Minimum Lane Changes is NOT available.

Table 4-5 is the version of Table 4-3 associated with the tree in Figure 4-4. Table 4-6 is the corresponding version of Table 4-4.

Table 4-5: Characteristics of the 11 terminal nodes in the tree not containing Minimum Lane Changes as a predictor of Total Lane Changes.

Node	Count	Mean	Standard Deviation
4	45	343.47	144.53
10	11	295.64	91.43
12	6	1713.00	334.49
13	19	2200.30	212.15
14	4	1897.50	400.35
22	10	286.80	75.14
30	24	2833.94	331.87
31	2	3816.00	441.23
46	14	988.29	292.03
94	94	1432.85	211.27
95	18	1879.18	198.14

Table 4-6: Cross-tabulation of sites and terminal nodes for the tree that does not include Minimum Lane Changes as a predictor of Total Lane Changes.

	Terminal Node											
Site	**4**	**10**	**12**	**13**	**14**	**22**	**30**	**31**	**46**	**94**	**95**	**Sum**
I-40 S Saunders E	8	0	0	0	0	1	0	0	6	1	1	17
I-40 S Saunders W	0	0	0	0	0	1	0	0	5	11	0	17
I-40/440 Basic EB	0	0	0	0	0	0	0	0	0	7	0	7
I-40/440 Basic WB	0	0	0	0	0	0	0	0	0	7	0	7
I-40/440 East Split	0	0	0	0	0	0	0	0	1	7	0	8
I-40WB WeaveE	0	0	0	0	0	0	0	0	0	10	0	10
I-40WB WeaveW	0	0	0	0	0	0	0	0	0	11	0	11
I-440 at Poole Rd E	0	0	0	0	0	0	0	0	0	7	0	7
I-440 at Poole Rd W	0	0	0	0	0	0	0	0	0	6	0	6
I-440 EB at Hillsborough Ext.	0	0	0	0	0	0	0	0	0	13	0	13
Ridge Rd	10	11	6	12	4	0	17	2	2	14	17	95
US101_Dnstrm	0	0	0	1	0	0	7	0	0	0	0	8
US101_Upstrm	0	0	0	6	0	2	0	0	0	0	0	8
US101_Wve	2	0	0	0	0	6	0	0	0	0	0	8
Wade WB at 440	25	0	0	0	0	0	0	0	0	0	0	25
Sum	45	11	6	19	4	10	24	2	14	94	18	247

The LCPT was validated by successively omitting each of the 15 sites, constructing a tree using data only from the 14 remaining sites, and comparing predicted values using that tree for data points from the omitted site with their actual values. Table 4-7 contains the results, but requires explanation:

- RMSE stands for Root Mean Squared Error, which for each site is the square root of the mean of the squared prediction error for Total Lane Changes, divided by the number of observations from that site.
- Relative RMSE is RMSE divided by the mean.
- There are three sets of predictions.
    - "No Model" corresponds to simply using the site mean as the predictor for the site. In effect, this approach assumes sites differ so much from one another that no "borrowing of strength" by means of a model is possible.[5]
    - "Full Model" corresponds to the model in Figure 4-3, which uses the data from all sites.
    - "Omitted Model" corresponds to the model described above, based on data from all sites other than that site.

Table 4-7: Validation results for model containing Minimum Lane Changes as a predictor of Total Lane Changes.

			RMSE			Relative RMSE		
Omitted Site	**Observations**	**Mean**	**No Model**	**Full Model**	**Omitted Model**	**No Model**	**Full Model**	**Omitted Model**
I-40 S Saunders E	17	1895.13	191.96	132.96	333.78	0.10	0.07	0.18
I-40 S Saunders W	17	2255.42	679.33	239.41	494.53	0.30	0.11	0.22
I-40/440 Basic EB	7	209.14	44.82	59.00	59.66	0.21	0.28	0.29
I-40/440 Basic WB	7	176.57	46.84	86.21	85.58	0.27	0.49	0.48
I-40/440 East Split	8	273.00	49.58	49.35	87.72	0.18	0.18	0.32
I-40WB Weave_E	10	420.00	160.50	143.81	139.84	0.38	0.34	0.33
I-40WB Weave_W	11	295.64	91.43	59.12	139.70	0.31	0.20	0.47
I-440 at Poole Rd E	7	2369.14	464.49	197.91	523.61	0.20	0.08	0.22
I-440 at Poole Rd W	6	2794.00	397.30	217.84	510.59	0.14	0.08	0.18
I-440 EB at Hillsborough Ext.	13	410.77	85.30	85.88	80.87	0.21	0.21	0.20
RidgeRd	95	1426.11	216.71	79.31	354.92	0.15	0.06	0.25
US101_Dnstrm	8	804.00	357.19	111.28	628.47	0.44	0.14	0.78
US101_Upstrm	8	402.00	124.54	115.41	274.44	0.31	0.29	0.68
US101_Wve	8	1113.00	408.69	135.33	1874.09	0.37	0.12	1.68
Wade WB at 440	25	2545.20	517.17	133.89	755.21	0.20	0.05	0.30

[5] As discussed below, this is demonstrably untrue.

In summary, the findings that arise from Table 4-7 are that:

1. With the exception of I-40/440 Basic EB, I-40/440 Basic WB, I-40/440 East Split Relative RMSE is uniformly lower for Full Model than No Model, which confirms that there is benefit from cross-site modeling.
2. Relative RMSE for Omitted Model is higher than[6] Relative RMSE for Full Model, but often only modestly so. This indicates that there is scientific generalizability for the modeling approach, which would be stronger if there were a greater variety of sites and more observations for each. The three US-101 sites are those for which the increase is most profound, which suggests that they are unlike the North Carolina sites.[7]

For the sake of completeness, Table 4-8 is the version of Table 4-7 for the model not containing Minimum Lane Changes as a predictor.

Table 4-8: Validation results for the model not containing Minimum Lance Changes as a predictor of Total Lane Changes.

			RMSE			Relative RMSE		
Omitted Site	**Observations**	**Mean**	**No Model**	**Full Model**	**Omitted Model**	**No Model**	**Full Model**	**Omitted Model**
I-40 S Saunders E	17	1895.13	191.96	186.91	1010.49	0.10	0.10	0.53
I-40 S Saunders W	17	2255.42	679.33	284.96	583.77	0.30	0.13	0.26
I-40/440 Basic EB	7	209.14	44.82	140.59	55.69	0.21	0.67	0.27
I-40/440 Basic WB	7	176.57	46.84	172.44	152.74	0.27	0.98	0.87
I-40/440 East Split	8	273.00	49.58	48.39	1052.02	0.18	0.18	3.85
I-40WB Weave_E	10	420.00	160.50	170.42	161.51	0.38	0.41	0.38
I-40WB Weave_W	11	295.64	91.43	87.18	1597.12	0.31	0.29	5.40
I-440 at Poole Rd E	7	2369.14	464.49	235.15	496.81	0.20	0.10	0.21
I-440 at Poole Rd W	6	2794.00	397.30	273.00	559.16	0.14	0.10	0.20
I-440 EB at Hillsborough Ext.	13	410.77	85.30	106.05	280.12	0.21	0.26	0.68
RidgeRd	95	1426.11	216.71	209.43	1169.67	0.15	0.15	0.82
US101_Dnstrm	8	804.00	357.19	242.46	1131.44	0.44	0.30	1.41
US101_Upstrm	8	402.00	124.54	130.38	878.29	0.31	0.32	2.18
US101_Wve	8	1113.00	408.69	301.75	934.55	0.37	0.27	0.84
Wade WB at 440	25	2545.20	517.17	307.48	904.49	0.20	0.12	0.36

[6] Or essentially equal to.
[7] The data for US-101, which are derived from NGSIM, also differ qualitatively from the directly observed North Carolina data.

4.4 Model Limitations

Below are the limitations of the lane change prediction models described above.

- The proposed models are not applicable to segment types that are not in the model development database such as ramp junctions with left-side entry or exit ramp. The models are also not applicable to sites consisting of multiple segments.
- Most sites in the database are weaving and basic freeway segments. It is recommended, if possible, to collect more data on merge and diverge segments to increase the generalizability of the models.
- The model, when applied to inputs that lie outside the range of values in the dataset, may produce unreliable results. The range of values for each independent variable is provided in Appendix B.

CHAPTER 5 : APPLY AND TEST TREATMENT EFFECTS

This chapter demonstrates the procedures and the results of testing a proposed treatment strategy to reduce lane change intensity at a weaving segment. The research team employed a microsimulation tool to evaluate the treatment's performance in terms of lane change and average travel time reduction. In addition, the research team developed a statistical tool called Simulated Annealing to assess the treatment's performance in terms of reducing lane change intensity using lane-based traffic counts.

The chapter begins with the description and the current operating condition of the site followed by the details of the proposed treatment strategy. Then the simulation study is described, including a data collection effort to calibrate the base scenario, modeling the treatment scenario, and comparing the performance of the two scenarios. Application of the Simulated Annealing method to evaluate the decrease in lane change frequency due to the treatment followed. The final section highlights the lessons learned from this task.

5.1 Background and Site Description

The initial plan of the research team was to select a site where a treatment for lessening lane change frequency had been implemented within the project timeline. However, within the radius within which a field survey is feasible for the research team, no treatment had been implemented during the project timeline. Rather, North Carolina Department of Transportation proposed a treatment for reducing lane change frequency at a busy weaving segment. The research team evaluated the proposed treatment strategy using microsimulation and statistical tools supplemented by necessary field data.

The proposed treatment site is more than a mile-long weaving segment located on Interstate 40 eastbound between N. Harrison Ave. and Wade Ave. near Raleigh, NC. Figure 5-1 shows the geometric properties of the site. There are already road signs and pavement marking at several points within and upstream of the segment telling which lanes exit and which continue on the interstate. Nonetheless, it experiences significant lane changing activities due to a great number of weaving traffic during the peak hours.

This freeway segment experiences heavy traffic demand during the PM peak as commuter traffic returns from the business zones in the Research Triangle Park to the residential zones in Raleigh. In addition, queue from two recurring bottlenecks located downstream of this segment degrade its mobility during the PM peak (Ahmed et al., 2018). These two bottlenecks are on downstream Interstate 40 and Wade Ave., with the later one having a higher severity. NCDOT hypothesized that this congestion impact is further magnified by the excess lane changing activities going on within the weave. This hypothesis is corroborated by the facts that the exiting traffic volume toward Wade Ave. – which is a major arterial – is very high (NCDOT, n.d.), and the merging traffic must make at least two lane changes according to the lane configuration (Figure 5-1).

These two mandatory lane changes might not have a serious mobility impact when the segment is so long, but when there are queued traffic on the rightmost lanes, these mandatory lane changes may create significant turbulence and trigger additional lane changing activities.

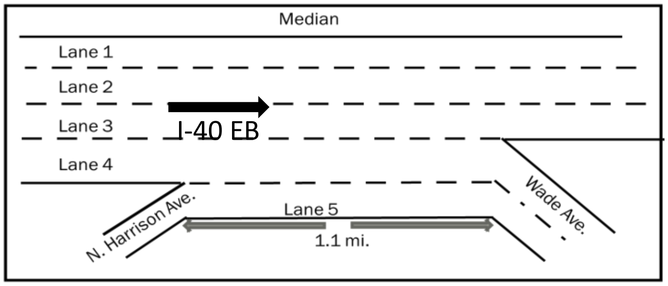

Figure 5-1: Current configuration of the study site

5.2 Proposed Treatment Strategy

To improve the current mobility of the study area, NCDOT proposed to add a lane 0.25 miles upstream of the entry gore as shown in Figure 5-2. This lane would continue through the entire weaving length and terminate 0.75 miles downstream of the exit gore. This proposed lane addition is expected to reduce the turbulence within the weave in several ways as follows.

- The proposed geometric changes would improve the speed of the freeway continuing traffic due to the added lane.
- It would increase the queue storage space for the exiting traffic.
- Lane change by freeway-to-ramp vehicles should decrease if proper guidance is provided for them to pre-position on the added lane upstream of the weave.
- Ramp-to-freeway vehicles would still have to make at least two mandatory lane changes for merging. However, it is reasonably expected that Lane 4 would be less occupied by other vehicles, which would reduce the turbulence effect of these mandatory lane changes.

Note that this proposed treatment is not for treating either downstream bottlenecks, rather its intended objective is to smooth the traffic operation within the weave.

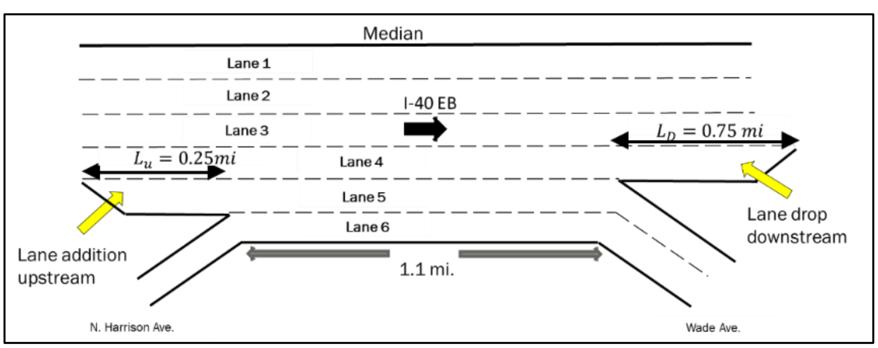

Figure 5-2: Proposed treatment configuration

5.3 Treatment Evaluation

The performance of the proposed treatment strategy is estimated using two techniques. One using a microsimulation tool and the other using a statistical tool called Simulated Annealing. For the later one, a required input is the entry vehicle count data by lane, which were obtained from the simulation model.

5.3.1 Evaluation Using Microsimulation

The research team used PTV VISSIM 10.0 (PTV, n.d.,) to test the effectiveness of the treatment because it is vastly used in past research for simulating traffic congestion and testing treatment effects (Gomes et al., 2004; Lee et al., 2013; Fan et al., 2013). Both existing (base) and proposed (treatment) scenarios are modeled in VISSIM. To collect origin-destination data and to calibrate the traffic stream speed of the base model, a field survey was conducted as described in the next section. Key parameter values for both models are:

- Runtime: 1 hr. following a 15-minute warm up period
- Number of runs: 7 in each scenario
- Input volumes (based on AADT data): 6,200 vehicles per hour from upstream freeway, 1,040 vehicles per hour from N. Harrison on-ramp, with 5% trucks
- Origin-destination proportions: Input volumes are adjusted by origin-destination proportions from the field data
- Lane change look up distance: This is the distance upstream of the exit gore from which a merging or diverging vehicle will try to make their mandatory lane changes. Based on the segment length and expected driving behavior, a value of 6,000 ft. was set from the exit gore for each mandatory lane change.

5.3.1.1 Field Data Collection

Field calibration data were collected using four Bluetooth detectors to capture sampled origin-destination volumes and sampled space mean speed and travel time. Four Bluemac x5 devices were deployed on roadside signposts which capture standard and low energy Bluetooth MAC addresses. One device was placed for each origin and destination as shown in Figure 5-3 and collected data from June 10 to June 14 2019.

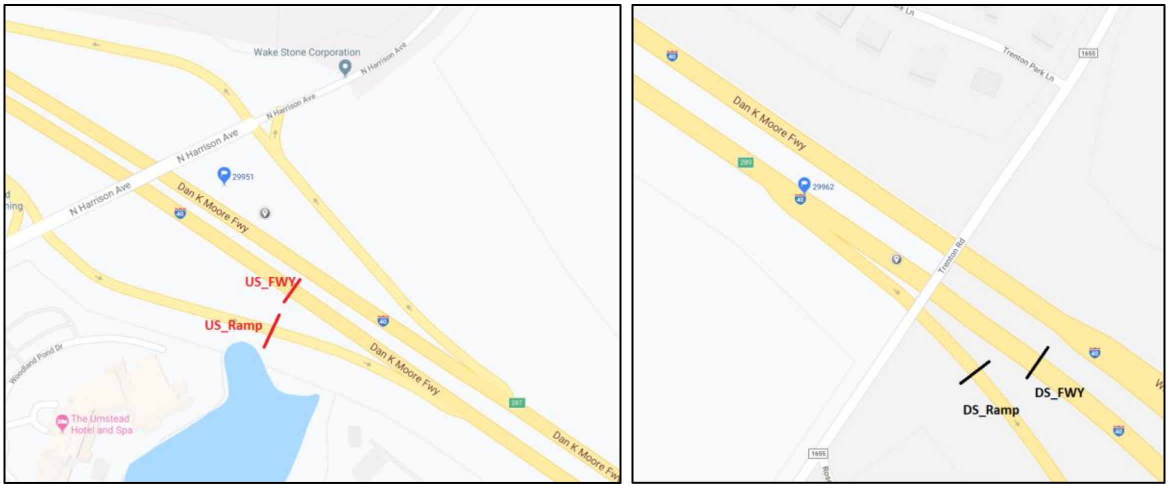

Figure 5-3: Field Calibration Data Collection Points

Two primary performance measures were collected to be utilized for microsimulation calibration. The first was the proportion of traffic travelling on each Origin to Destination pair. The proportion of traffic was utilized rather than the directly measured volume as Bluetooth sensors only collect a sample of total traffic, usually varying between 4-15% depending on the facility type and region. Data were summarized at the hourly level for each weekday for checking for data quality issues, which found that peak period patterns were most consistent on Tuesday, Wednesday and Thursday. The PM peak period of 4-6 PM is summarized in Table 5-1, showing similar distributions though the ramp traffic was lower overall on Thursday 6/13. In the naming, F represents Freeway and R represents Ramp with the first letter indicating the origin and the second the destination. The mean proportions used for freeway originating traffic is 46% to freeway and 54% to off-ramp, and for on-ramp originating traffic is 32% to freeway and 68% to off-ramp.

Table 5-1: Field Sampled Origin to Destination Volumes (4-6 PM)

Day	FF	FR	RF	RR
Tue, 6/11	2190	2567	678	1380
Wed, 6/12	2478	2821	693	1399
Thu, 6/13	2253	2606	449	1018

The second performance measure of interest is the sampled travel time for each O-D pair. As this performance measure can vary greatly in consecutive time periods, a five-minute average travel time was calculated for each O-D pair for the three typical weekdays. This resulted in a sample size of between 70 to 130 trips sampled in each 5 minute period during the PM peak period of 4-6PM. Initial discussion with NCDOT identified two separate areas of congestion, the first on the off-ramp with downstream queues impacting the speed and throughput of the off-ramp and secondly downstream on the freeway where a smaller speed drop is observed due to congestion at the downstream interchange. Figure 5-4 shows the average travel time for Freeway to Ramp trips with travel time increasing over 100% higher during peak congestion compared to uncongested time periods. Figure 5-5 shows that the Freeway downstream congestion had a smaller overall impact on travel time however the peak 5-minute period was slightly later than the ramp congestion. These two specific patterns were noted for use in the calibration shown in the next section.

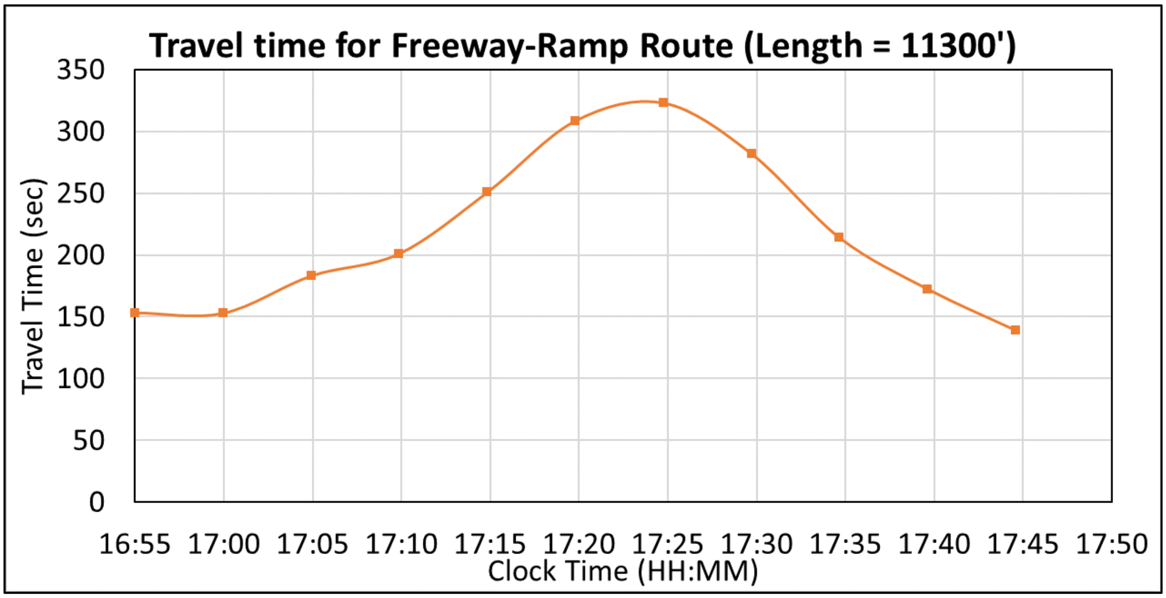

Figure 5-4: Average 5-minute Freeway to Ramp Travel Time (PM Peak)

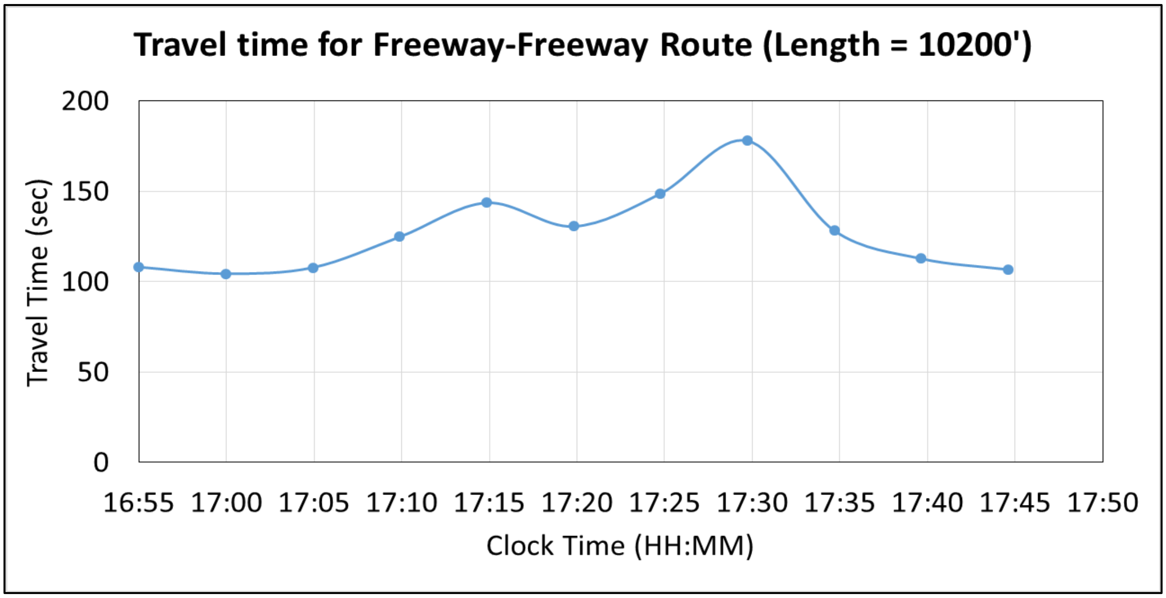

Figure 5-5: Average 5-minute Freeway to Freeway Travel Time (PM Peak)

5.3.1.2 Base Model Calibration

While modeling the current geometry and origin-destination flow rates in VISSIM was straightforward with the available mapping tools and field data, simulating the two bottleneck effects were not trivial. Some common ways of simulating traffic congestion as described in previous studies are:

- By changing driver behavior parameters (Gomes et al., 2004)
- By introducing an artificial lane drop (Lee et al., 2013)
- By introducing reduced speed areas (Fan et al., 2013)

The research team attempted all these techniques to simulate the congested condition and calibrate the model against field travel time data during PM peak. The third technique, which is by introducing reduced speed areas gave the best calibration performance. Reduced speed areas were modeled on downstream Wade Ave. and Interstate 40 and their severity was selected by calibrating against the field data. In addition, their severity was raised with time to mimic field observations. Field data on travel time to traverse different pairs of Bluetooth sensors during the PM peak hours are averaged over multiple weekdays. This average travel time data for 1 hour of PM peak period, which was from 5 pm to 6 pm, were used to calibrate the VISSIM simulated travel time data. Figure 5-6 shows the cumulative distribution of average travel time estimated from Bluetooth readings (marked as "BT") and from simulation runs (marked as "VISSIM") for different origin destination routes. Each data point in these distributions represents a 5-minute aggregated average travel time per vehicle.

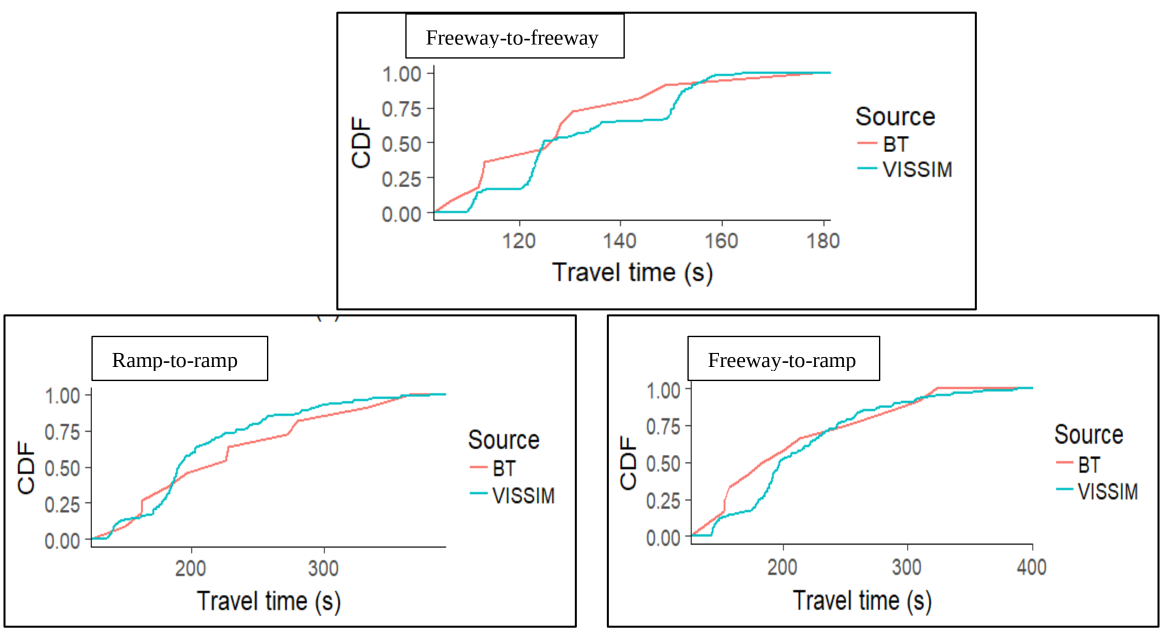

Figure 5-6: Calibration of travel time for different origin-destination routes

Note that the travel time distribution for the ramp-to-freeway route are not shown here as this route has the least flow rate and the impact of the treatment is also expected to be the least along this route. Travel time distributions for the remaining three routes in Figure 5-6 show that the deviation between the VISSIM simulated and field-observed travel time distributions is small. The freeway-to-freeway route exhibits the highest deviation, where the difference in the mean of these two distributions is 15 seconds.

5.3.1.3 Treatment Scenario Model

The proposed geometric improvement as shown in Figure 5-2 was modeled in VISSIM, while keeping the traffic volume and other simulation parameters same as in the base model. The severity of the bottleneck on downstream Interstate 40 is expected to drop due to the lane addition, but the magnitude of this reduction is unknown. Hence, two treatment scenarios were generated. In the more conservative approach, the severity of that bottleneck was kept same as in the base model i.e., its severity was raised with time, while in another one its severity was remained constant with time. Being more agreeing with the expected reduction in severity, results from the later one are presented here.

5.3.1.4 Comparison of Base and Treatment Scenario

To compare the performance of the proposed treatment, average travel times aggregated in 5-minute interval are estimated for one-hour of PM peak for both scenarios. For comparison of the scenarios, travel time was measured as the time required to travel from the point of lane addition upstream of the weave to the point of terminating that lane downstream of the weave (Figure 5-2). Furthermore, lane change frequency within the weave was compared between these two scenarios.

Figure 5-7 shows the cumulative distribution of average travel time for the base (shown as "BASE") and the treatment (shown as "TRTMNT") scenario. Each data point in these distributions represents a 5-minute aggregated average travel time per vehicle. There are 84 data points in each distribution (7 simulation runs times 12 intervals in 1 hour).

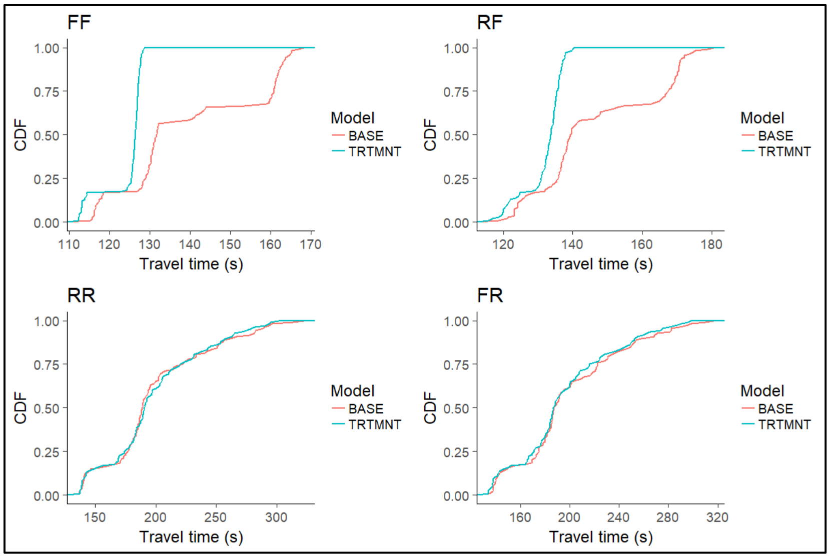

Figure 5-7: Comparison of the travel time distribution between base and treatment scenario by origin-destination routes

It is apparent from Figure 5-7 that the travel time distributions are almost identical between the two scenarios for the ramp-to-ramp and freeway-to-ramp routes, implying that these two routes are gaining little to no benefit of the treatment. The main reason behind it is that the average travel time for vehicles that are exiting toward Wade Ave. is mainly governed by the downstream bottleneck on the Wade Ave. Since the treatment is not interacting with that bottleneck, no impact is seen on the travel time distribution for the exiting vehicles.

Conversely, the travel time distributions for vehicles that are continuing on the interstate have shifted toward left in the treatment scenario. It indicates that the lane addition is helping the freeway continuing traffic to be isolated from the impact of the queue emanating from the Wade Ave. bottleneck.

Table 5-2 shows the treatment effect in terms of travel time saving for all vehicles along different origin-destination routes. Further analysis of the Bluetooth sample trip counts indicate that the estimated travel time savings in one hour should be applied to two hours of PM peak at this segment, implying that the travel time savings reported in Table 5-2 would be double for the PM peak for a typical weekday.

Table 5-2: Travel time savings by the proposed treatment for different routes

Route type	Travel time saving in 1 hour (veh-hrs.)
Freeway-freeway	12.7
Freeway-ramp	1.9
Ramp-freeway	1.4
Ramp-ramp	0.2

Analysis of the lane change data revealed that the total lane change frequency during the peak hour was reduced by 22% in the treatment scenario. Origin-destination based analysis showed that this reduction was primarily contributed to the pre-positioning of the freeway-to-ramp vehicles and less discretionary lane changes by the freeway-to-freeway vehicles.

5.4 Evaluation using Simulated Annealing

This section explains an alternate approach for evaluating a treatment effect in terms reduction in lane change frequency. The motivation was to develop a statistical tool that can readily assess the difference in lane change distribution before and after a treatment without having to model both scenarios in a microsimulation environment. To demonstrate, lane-by-lane entry and exit vehicle count data from the simulation runs for both base and proposed models were employed.

5.4.1 Comparing Baseline and Treatment

The lane-by-lane baseline origin-destination matrix is given in Table 5-3. On the assumption that a vehicle with origin lane i and destination lane j makes $|i-j|$ lane changes, there are 5152 lane changes for the baseline scenario. Similarly, in the treatment scenario, for which the origin-destination matrix appears in Table 5-4, there are 4307 lane changes. While the 16% reduction in lane changes appears substantial, there remains the question of whether it is, even partly, the consequence of VSSIM-associated randomness.

Table 5-3: Baseline origin-destination matrix

	Destination Lane					
Origin Lane	**1**	**2**	**3**	**4**	**5**	**Sum**
1	559	232	98	0	0	889
2	381	476	215	0	1	1073
3	103	183	322	600	263	1471
4	69	107	146	1091	1038	2451
5	58	86	124	267	752	1287
Sum	1170	1084	905	1958	2054	7171

Table 5-4: Treatment origin-destination matrix.

	Destination Lane						
Origin Lane	**1**	**2**	**3**	**4**	**5**	**6**	**Sum**
1	547	215	68	22	0	0	852
2	184	542	127	33	1	0	887
3	36	114	432	84	18	5	689
4	5	29	110	224	384	159	911
5	7	12	31	53	1330	1126	2559
6	11	32	90	153	240	757	1283
Sum	790	944	858	569	1973	2047	7181

There is no formal statistical test for assessing the difference in lane changes. We addressed the issue by generating 1,000,000 "nearby" (defined momentarily) tables for the baseline scenario, each with the same row and column marginals (sums) as the O-D matrix in Table 5-3; generating 1,000,000 "nearby" tables for the treatment scenario, each with the same marginals as the O-D matrix in Table 5-4Table 5-4, then comparing the distributions of the numbers of lane changes. The nearby tables were further constrained to preserve small cell counts (zeros and ones), as well as to match approximately the freeway/ramp O-D matrices.[8]

Nearby tables result from applying *Markov bases* from the field of computational algebraic statistics. The seminal reference is Diaconis and Sturmfels (1998). The fundamental concept of *adjacency* for two tables is illustrated in the following example. To the leftmost table is added a table with exactly four non-zero entries, two of which are 1 and the other two of which are -1, arranged so that the row and column marginals are both 0. The resultant table, which therefore has the same row sums as the original table, is on the right-hand side of the equation. In a clear sense, it is adjacent to the initial table.

$$\begin{bmatrix} 15 & 4 & 3 & 1 \\ 4 & 20 & 5 & 2 \\ 2 & 5 & 18 & 5 \\ 1 & 0 & 5 & 17 \end{bmatrix} + \begin{bmatrix} -1 & 0 & 1 & 0 \\ 0 & 0 & 0 & 0 \\ 1 & 0 & -1 & 0 \\ 0 & 0 & 0 & 0 \end{bmatrix} = \begin{bmatrix} 14 & 4 & 4 & 1 \\ 4 & 20 & 5 & 2 \\ 3 & 5 & 17 & 5 \\ 1 & 0 & 5 & 17 \end{bmatrix}.$$

The 1,000,000 tables for each scenario were generated by performing 5000 Markov basis moves (subject to the constraints described above), and re-starting the process 200 times, in order to ensure full exploration of the set of nearby O-D matrices with the same marginals. The number of lane changes for each table was calculated, and the two distributions compared, with the result shown in Figure 5-8. There is virtually no overlap between the two distributions, so the difference is indeed significant. (There is literal overlap, but it is insignificant. The minimum number of lane changes for the baseline scenario, over 1,000,000 tables, is 4786, which lies at the 99.75th percentile of the treatment distribution, while the maximum number of lane changes for the treatment scenario is 4885, and lies at the .26th percentile of the baseline distribution.)

[8] And, of course, to have nonnegative entries.

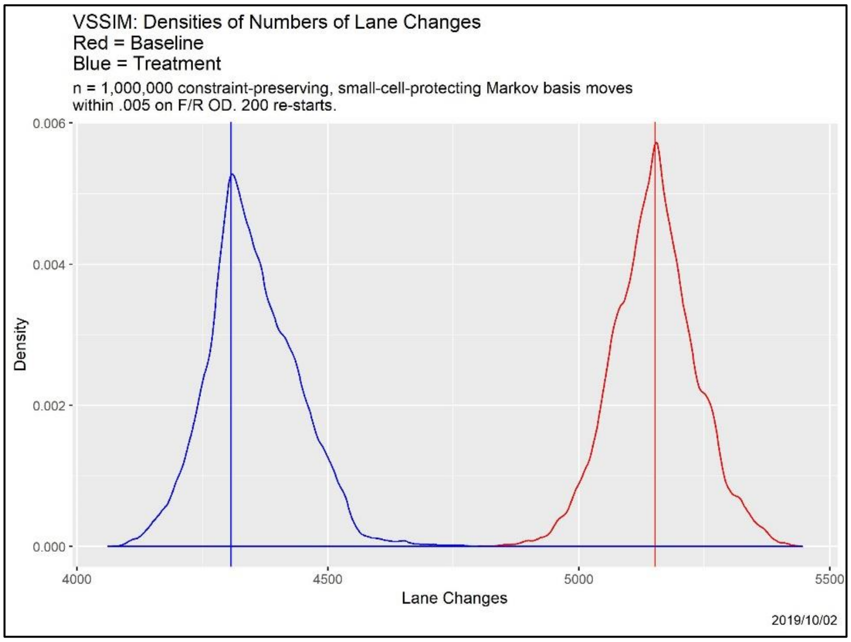

Figure 5-8: Comparison of the density functions of numbers of lane changes for the baseline and treatment scenarios.

5.5 Lessons Learned

The key lessons learned from testing the treatment effects are highlighted below

- From the simulation experiment, it was found that the travel time reduction by the treatment highly depends on the effect of the treatment on the downstream freeway bottleneck. The expected travel time saving ranges from 5.7 to 16.2 veh-hours per clock hour of peak period, depending on whether the treatment will have no or a strong effect, respectively, on the downstream I-40 bottleneck.
- Creating traffic congestion in VISSIM is not as straightforward as only loading the model with sufficient vehicles. While the most appropriate method, which is adding reduced speed areas, is applied in this study, other methods like changing driver behavior parameters or a combination of these are worth exploring.
- Lane change look-up distance has a significant impact on merging and diverging behavior. The most appropriate values were used here depending on the traffic and geometric characteristics of the model, so that no unrealistic queue forms at the lane addition point.

CHAPTER 6 : DEVELOP TOOL FOR NCDOT USE

The LCPT software tool is a password-protected, web-based application for predicting total hourly lane change counts in IIAs from four segment characteristics and four hourly traffic stream values. *The tool treats traffic in one direction only*. The prediction is accompanied by an estimate of the associated uncertainly as well confidence bounds. The primary output to the user is a record of the inputs and results. The underlying statistical methodology is partition trees (described in Chapter 4), as implemented in the **`rpart`** package of the R software environment. The web interface was built using the **`shiny`** and **`knitr`** packages. Employing the LCPT requires only a network connection and web browser.

The LCPT consists of a single screen, whose components are described in turn. First, there is a header containing links to download three files—the LCPT User Guide (PDF format); an Excel spreadsheet that assists in calculating two inputs—Minimum Lane Changes and Space Mean Speed; and the ReadMe file for the calculator (PDF format). This ReadMe file is also provided in Appendix C of this report.

Next, there is a required *Case Identifier*, which distinguishes the case under study and is used to name files. Then, there are four optional variables containing *Project Information*: the name and firm/unit of the analyst; a project name or number; and the information that describes the site.

The principal inputs to the LCPT, as shown in Figure 6-1, are:

- Four required *Segment Variables*—Segment Length, Number of Lanes, Distance to the Nearest On-Ramp, and Distance to the Nearest Off-Ramp;
- Four required (uni-directional) *Hourly Traffic Variables*—Total Flow Rate. Heavy Vehicle Percentage, Minimum Lane Changes and Average Speed.

All input variables are numerical, and the LCPT software tool generates an error message whenever a user-entered value is missing or invalid. The downloadable spreadsheet calculator may be used, if desired, to assist in calculating Minimum Lane Changes and Average Speed. As shown in Figure 6-1, for each variable, there is a link to information about it.

By default, the software tool uses the partition tree model containing Minimum Lane Changes as a predictor of Total Lane Changes (Section 4.2). If, even with the assistance of the spreadsheet calculator, no value of this input can be calculated, then the user enters xxx, which causes the tool to use the partition tree model NOT containing Minimum Lane Changes as a predictor of Total Lane Changes.

When the user clicks the Calculate/Report button in Figure 6-2, then (assuming inputs are valid), the software tool uses the appropriate partition tree model (Section 4.2 and 4.3) to calculate the predicted value of Hourly Total Lane Changes, the approximate standard error, and the confidence bounds, which are displayed on-screen as shown in Figure 6-2. As also shown there, the software tool generates a downloadable PDF report that contains the inputs, outputs, and a graphical representation of the path through the appropriate partition tree, as shown in Figure 6-3. An example PDF report accompanies this report.

The software tool permits users to enter inputs that lie outside the range of values in the dataset. When this happens, the tool will produce results and generate the PDF report. However, those results may not be reliable, and the user is warned to this effect in both screen output and the PDF report.

A complete description of the software tool is contained in the downloadable User Guide, which also accompanies this report.

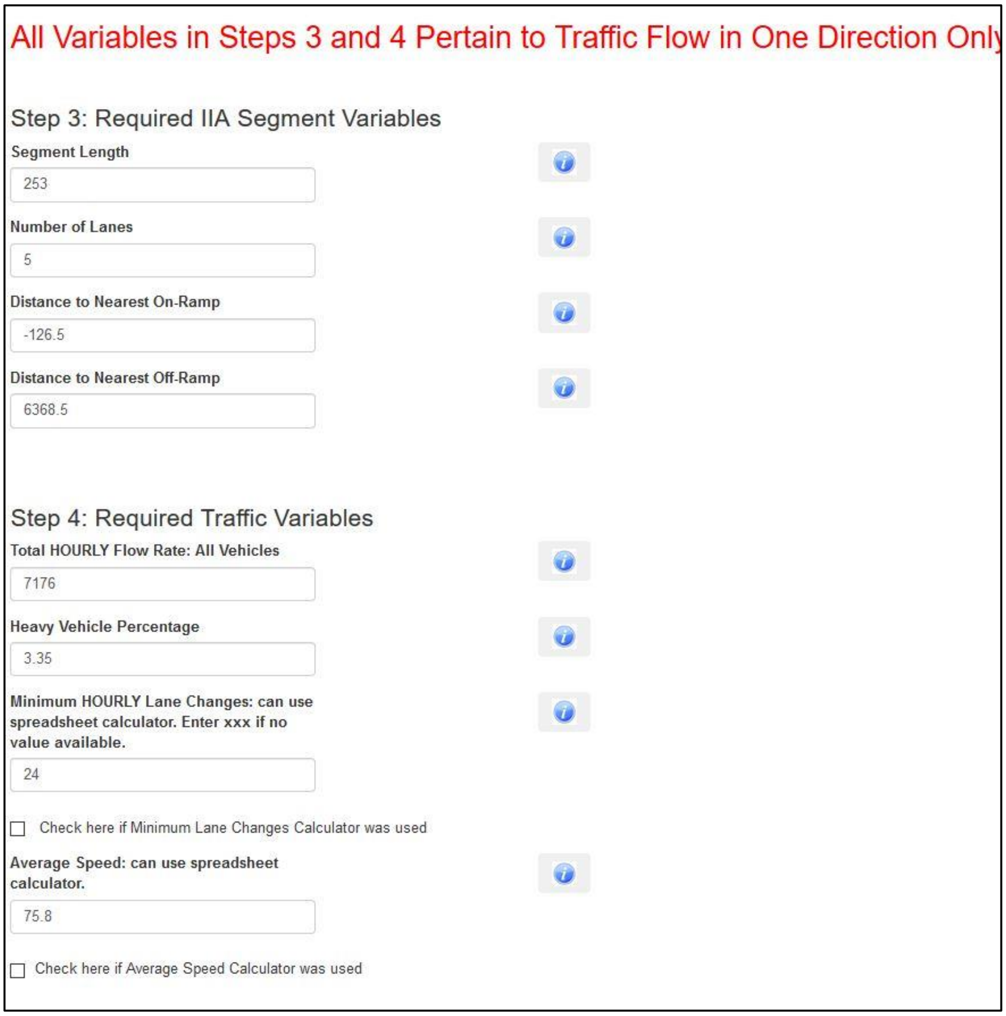

Figure 6-1: Segment Variable and Hour Traffic Variable inputs to the LCPT software tool

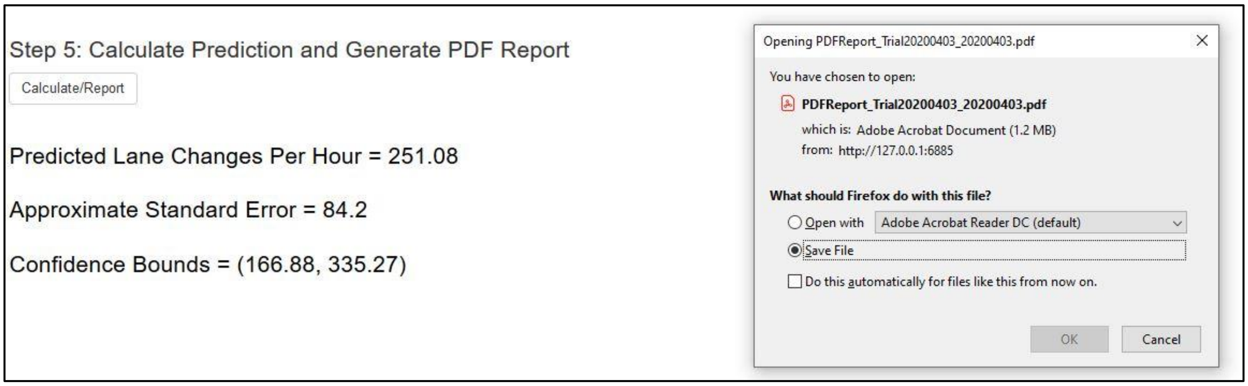

Figure 6-2: LCPT on-screen results for the inputs shown in Figure 6-1.

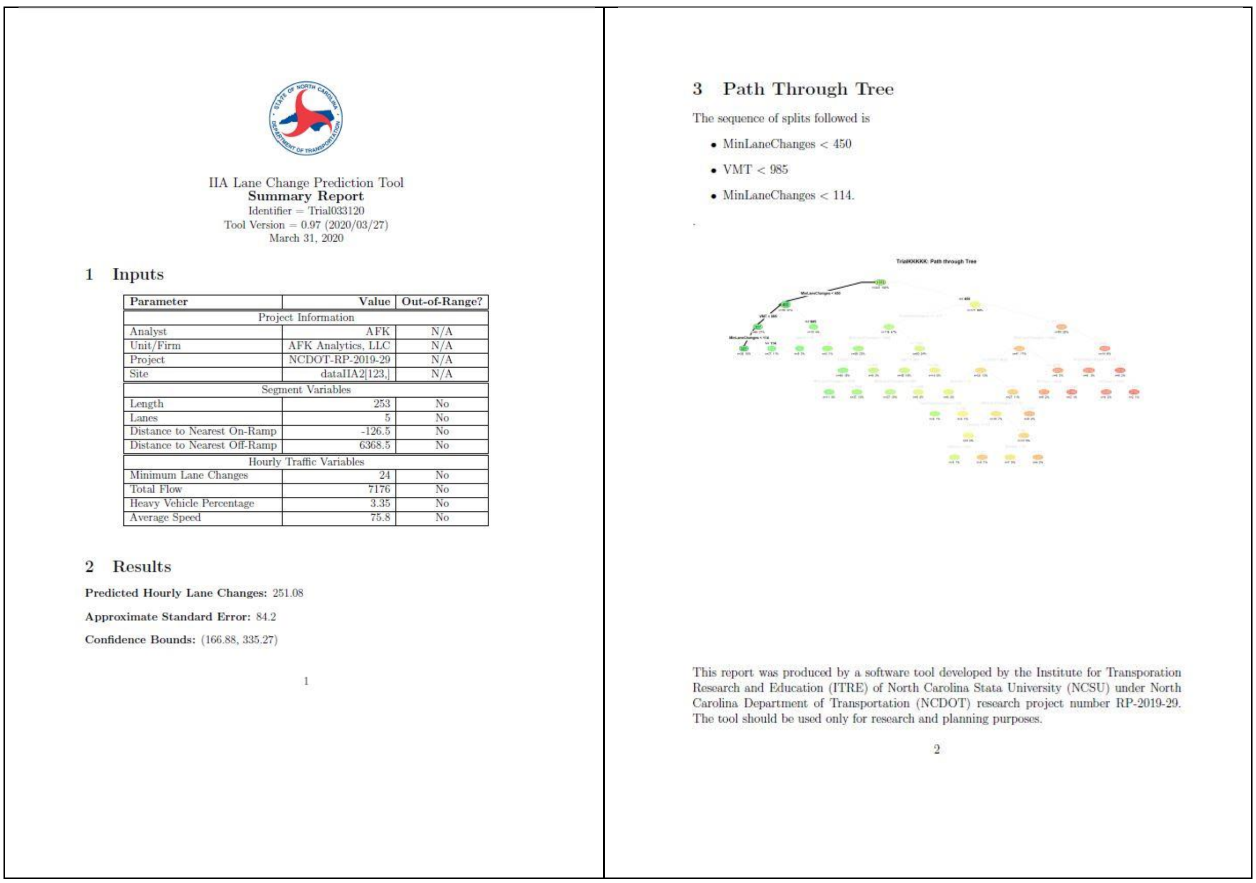

IIA Lane Change Prediction Tool
Summary Report
Identifier = Trial033120
Tool Version = 0.97 (2020/03/27)
March 31, 2020

1 Inputs

Parameter	Value	Out-of-Range?
Project Information		
Analyst	AFK	N/A
Unit/Firm	AFK Analytics, LLC	N/A
Project	NCDOT-RP-2019-29	N/A
Site	dataIIA2[123,]	N/A
Segment Variables		
Length	253	No
Lanes	5	No
Distance to Nearest On-Ramp	-126.5	No
Distance to Nearest Off-Ramp	6368.5	No
Hourly Traffic Variables		
Minimum Lane Changes	24	No
Total Flow	7176	No
Heavy Vehicle Percentage	3.35	No
Average Speed	75.8	No

2 Results

Predicted Hourly Lane Changes: 251.08

Approximate Standard Error: 84.2

Confidence Bounds: (166.88, 335.27)

1

3 Path Through Tree

The sequence of splits followed is

- MinLaneChanges < 450
- VMT < 985
- MinLaneChanges < 114.

.

TrialXXXXX: Path through Tree

This report was produced by a software tool developed by the Institute for Transporation Research and Education (ITRE) of North Carolina Stata University (NCSU) under North Carolina Department of Transportation (NCDOT) research project number RP-2019-29. The tool should be used only for research and planning purposes.

2

Figure 6-3: PDF report associated with the inputs in Figure 6-1

CHAPTER 7 : SUMMARY, CONCLUSIONS, AND RECOMMENDATIONS

7.1 Summary

This research project aims at providing the North Carolina Department of Transportation with a computational tool for predicting the lane change intensity near Interchange Influence Areas (IIAs). The intent was to use data that are readily available to traffic engineers and analysts in the state to generate those predictions. This research is motivated by several factors, including: (a) the documented turbulence caused by unnecessary lane changing at IIAs, (b) the inability of traditional traffic detection systems to quantify lane change intensity and (c) the need to assess whether specific treatments aimed at reducing unnecessary lane changes are effective. To that end, the research distinguishes between "*mandatory*" --- or the minimum number of ---lane changes that must be made to reach one's destination (i.e. to merge, diverge or weave), and those lane changes made while maintaining one's current course, or "*discretionary*". The proposed tool estimates the combined number of lane changes using two different models, one that assumes knowledge of the number of the mandatory lane changes, and a second model that does not. The first model applies to existing interchange areas where ramp volumes are known, while the second can be used for new interchange analyses at the planning stage.

Data needed to develop the prediction tool included both geometric and traffic variables. A total of fifteen sites were videotaped using a combination of ground based and (mostly) drone fitted cameras, mostly in the Research Triangle Region. The majority of the data collection sites were of the weaving segment category where both on ramp and off ramp vehicular traffic intermingle in a confined space, generating multiple mandatory and discretionary lane changes. Data were also collected at a diverge segment, and at a number of basic segment locations where all lane changes are considered to be discretionary. Data extraction from videos was carried out using a combination of manual processing and checking, and automated vehicle tracking methods. Data From Sky (DFS), a third party vendor produced "processed" drone videos which allowed the research team to accurately measure lane change counts and other traffic parameters such as speed, passenger car and heavy vehicle volume collected at each site. Subsequently, a fused database combining all observations from all sites, was developed containing five-minute measurements of traffic and site variables for a specific segment location. All counts of traffic volumes and lane changes were expressed in terms of hourly rates.

All in all, the fused database contained 247 observations from which a predictive lane change model could be developed. Documentation of the database is provided in Appendix A. Finally, the fused data was used towards the development of two Classification and Regression Tree (CART) models based on the availability of the minimum lane change frequency rate per hour, as described in the next section. The two models are currently being implemented through a web-based computational tool that will reside on one of ITRE's servers. A prototype tool has been developed, along with a user guide and input calculator. It was recently demonstrated to the NCDOT StIC Committee. The research team anticipates completing and successfully testing of the web based tool at some point during the Fall Semester 2020 once the NC State campus is universally accessible.

7.1.1 Key Findings from Predictive Models

Regression trees are different from traditional linear regression models in that they do not assume that the response variable, in this case the total rate of lane changes per hour, is linearly correlated with the predictor variables, for example volume or speed. On the other hand, the values of the response variables are not continuous, but are discrete, and their value displayed at the terminal nodes of the tree. To determine the optimal number of terminal nodes (or solutions), the algorithm partitions the original dataset into a train and a test set by taking random samples iteratively, and selects the one that minimizes the error of applying the trained model on the test dataset. Additionally, a minimum number of observations at each terminal node were specified as a constraint. In addition to the expected number of overall lane changes per hour, the model gives an estimate of the standard deviation of the mean, so that the user has an idea of the likely range of the response variable at each terminal node.

Overall, the average number of lane changes across all the sites and time intervals was 1,373 lane changes per hour. The validation of the tree prediction models was carried out by successively omitting the lane change data from each of the 15 sites, and constructing a tree using data only from the 14 remaining sites (this process is termed as “Omitted Model”). We then compare the predicted values using that second tree for data points from the omitted site with their actual values. That validation was deemed to be successful for most sites. Key findings from the first tree in which the minimum number of lanes changes (MinLaneChanges) is known are summarized as follows:

1. The tree contained 22 terminal nodes each giving a prediction based on a sequence of binary choice of variable values in the model.
2. The range of the response variable varied from a low of 251 to a high of 3,798 lane changes per hour
3. Generally speaking, low rates of lane changes were associated with low values of MinLaneChanges, low vehicle miles of travel (VMT), and low average speed.
4. Unsurprisingly, the first explanatory variable in the tree was MinLaneChanges, with a threshold MinLaneChanges=450 per hour discriminating between low and high lane change conditions.
5. The next set of splits is explained by the distance to the nearest on ramp. A threshold value of 417 feet was the boundary between low and high lane change rates
6. Other variables appearing in the tree include Passenger car flow rate, Density and Total Flow Rate per lane.

7. The relative root mean square error (Error /Mean Value, or RMSE) varied from a low of 0.05 up to 0.49 for different sites, with the highest value—unsurprisingly, occurring on a basic segment.
8. With the exception of I-40/440 Basic EB, I-40/440 Basic WB, I-40/440 East Split Relative RMSE is uniformly lower compared to a No Model case for all other sites, which confirms that there is benefit from cross-site modeling.

Similarly, key findings from the second tree in which the minimum number of lanes changes (MinLaneChanges) was not available are summarized as follows:

1. The tree contained only 11 terminal nodes each giving a prediction based on a sequence of binary choice variables in the model.
2. In general the RMSE values for this model were higher than the model with known MinLaneChanges.
3. The range of the response variable varied from a low of 343 to a high of 3,816 lane changes per hour
4. Generally speaking, low rates of lane changes were associated shorter segment lengths, within a short distance downstream of an on-ramp, at low passenger car flow rates and low speeds.
5. The first explanatory variable in the tree absent MinLaneChanges was the actual segment length, with longer segments generating higher lane change rates. The threshold length value dividing high and low rates was 910 ft.
6. The next set of splits is explained by the total flow rate per lane, with lower flow rates yielding fewer lane changes. It should be made clear that low flow rates will occur under both free flow and highly congested conditions. Our observations of the data is that lane changes decrease as congestion increases.
7. Other variables appearing in the tree include Passenger car flow rate, Density and total flow rate per lane.
8. The relative root mean square error (Error /Mean Value, or RMSE) varied from a low of 0.1 up to 0.98 for different sites, with the highest value—unsurprisingly, occurring on a basic segment.

7.1.2 Key Findings from Treatment Effect

As described in Chapter 5, the research team tested a proposed treatment at the I-40 EB weaving segment between N. Harrison Ave. and Wade Ave. The initial testing was intended to be carried out in simulation, and if it met the SPOT mobility criteria would have been recommended for field implementation. The aim was to relieve the current congested condition at the site by changing its lane configuration, which is expected to reduce the lane change intensity and reduce average travel time through the site during the PM peak. The testing method was a combination of microsimulation using a calibrated VISSIM model based on observed OD flow distributions and travel times measured from field Bluetooth units. The model outcome were tested with a series of Markov Base moves to predict the distribution of lane changes before and after the treatment was implemented in simulation. Key findings from this work include:

1. The treatment generated total travel time saving 16.2 veh-hours per clock hour, which is applicable to two hours of PM peak on a typical weekday. Those values, however, did not meet the threshold for field implementation
2. The treatment reduced the overall lane change frequency by a significant 22%.
3. The Markov bases tool revealed a clear distinction between the lane change frequency distributions for the base and the treatment scenarios with under .05 percent overlap between the two.

7.2 Recommendations for Future Work

We offer the following recommendations for future work aimed at enhancing the predictive abilities of the proposed models:

1. As additional data, similar to the one available in the fused dataset become available, both regression trees can be readily re-fitted and their predictive ability improved.
2. When such additional data become available, data-rich models that focus on predicting discretionary lane changes (only) should be advanced.
3. Weaving segments were, understandably, the dominant segment type in this study. Data collected at additional merge and diverge segments would improve the generalizability of the model findings
4. Sites with configurations not considered in this study, including two-sided weaves and combination of multiple segments are not covered here and recommended for future studies
5. Should a field treatment aimed at reducing the frequency of lane changes be considered by NCDOT, the team recommends a site from the list of NC sites used in this study. This will make the before (or base) condition data be available to test the treatment effects.

CHAPTER 8 : REFERENCES

Ahmed, I., Rouphail, N. M., & Tanvir, S. (2018). Characteristics and temporal stability of recurring bottlenecks. Transportation research record, 2672(42), 235-246.

Breiman, L., Friedman, J., Stone, C. J., & Olshen, R. A. (1984). Classification and regression trees. CRC press.

Chang, G., & Kao, Y. (1991). An empirical investigation of macroscopic lane-changing characteristics on uncongested multilane freeways. *Transportation Research Part A: General, 25*(6), 375-389.

Chen, D., & Ahn, S. (2018). Capacity-drop at extended bottlenecks: Merge, diverge, and weave. *Transportation Research Part B: Methodological, 108*, 1-20.

Daganzo, C. F., Laval, J., & Munoz, J. C. (2002). Ten strategies for freeway congestion mitigation with advanced technologies. *California Partners for Advanced Transit and Highways (PATH),*

DataFromSky (n.d.). Retrieved from https://ai.datafromsky.com/aerial

Diaconis, P., & Sturmfels, B. (1998). Algebraic algorithms for sampling from conditional distributions. The Annals of statistics, 26(1), 363-397.

Fan, R., Yu, H., Liu, P., & Wang, W. (2013). Using VISSIM simulation model and Surrogate Safety Assessment Model for estimating field measured traffic conflicts at freeway merge areas. IET Intelligent Transport Systems, 7(1), 68-77.

FHWA, M. (2009). Manual on uniform traffic control devices.

Gan, Q., & Jin, W. (2015). Left-lane changes in laterally unbalanced traffic: Estimating number of lane changes with data from lane-based loop detectors. *Transportation Research Record: Journal of the Transportation Research Board,* (2490), 106-115.

Gomes, G., May, A., & Horowitz, R. (2004). Congested freeway microsimulation model using VISSIM. Transportation Research Record, 1876(1), 71-81.

Goodvision (n.d.). Retrieved from https://goodvisionlive.com/

Knoop, V., Hoogendoorn, S., Shiomi, Y., & Buisson, C. (2012). Quantifying the number of lane changes in traffic: Empirical analysis. *Transportation Research Record: Journal of the Transportation Research Board*, (2278), 31-41.

Laval, J. A., & Daganzo, C. F. (2006). Lane-changing in traffic streams. *Transportation Research Part B: Methodological, 40*(3), 251-264.

Lee, J., Dailey, D. J., Bared, J. G., & Park, B. B. (2013). Simulation-based evaluations of real-time variable speed limit for freeway recurring traffic congestion (No. 13-4329).

Lee, J., Park, M., & Yeo, H. (2016). A probability model for discretionary lane changes in highways. *KSCE Journal of Civil Engineering, 20*(7), 2938-2946.

Manual, H. C. (2010). Hcm2010. *Transportation Research Board, National Research Council, Washington, DC,*

Moridpour, S., Sarvi, M., & Rose, G. (2010). Modeling the lane-changing execution of multiclass vehicles under heavy traffic conditions. *Transportation Research Record: Journal of the Transportation Research Board,* (2161), 11-19.

NCDOT (n.d.). Retrieved from https://connect.ncdot.gov/resources/State-Mapping/Pages/Traffic-Volume-Maps.aspx

NGSIM homepage. (2006). Retrieved from https://www.its-rde.net/index.php

Roess, R., & Ulerio, J. (2009). Level of service analysis of freeway weaving segments. *Transportation Research Record: Journal of the Transportation Research Board,* (2130), 25-33.

Sala, M., Soriguera, F., Huillca, K., & Vilaplana, V. (2019). Measuring traffic lane-changing by converting video into space–time still images. Computer-Aided Civil and Infrastructure Engineering, 34(6), 488-505.

Schakel, W. J., Knoop, V. L., & van Arem, B. (2012). Integrated lane change model with relaxation and synchronization. *Transportation Research Record, 2316*(1), 47-57.

Singh, K., & Li, B. (2012). Estimation of traffic densities for multilane roadways using a markov model approach. *IEEE Transactions on Industrial Electronics, 59*(11), 4369-4376.

Soekroella, A., Hegyi, A., Hoogendoorn, S. P., & van Kooten, J. (2012). Dynamic lane separation to prevent blocking back-A comparison of two dynamic lane separation controllers. Paper presented at the *Intelligent Transportation Systems (ITSC), 2012 15th International IEEE Conference On,* 1032-1037.

Spiliopoulou, A., Papageorgiou, M., Herrera, J. C., & Muñoz, J. C. (2016). Real-time merging traffic control at congested freeway off-ramp areas. *Transportation Research Record: Journal of the Transportation Research Board*, (2554), 101-110.

Thiemann, C., Treiber, M., & Kesting, A. (2008). Estimating acceleration and lane-changing dynamics from next generation simulation trajectory data. *Transportation Research Record: Journal of the Transportation Research Board*, (2088), 90-101.